

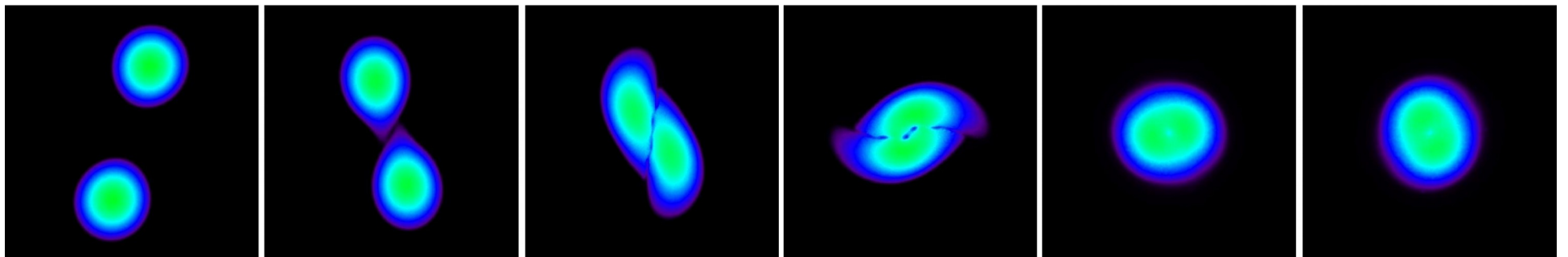
Neutron Star Mergers

Andreas Bauswein

Heidelberg Institute for Theoretical Studies

Nuclear Theory and Astrophysical Applications

JINR - July 19, 2017, Dubna



Neutron-star mergers

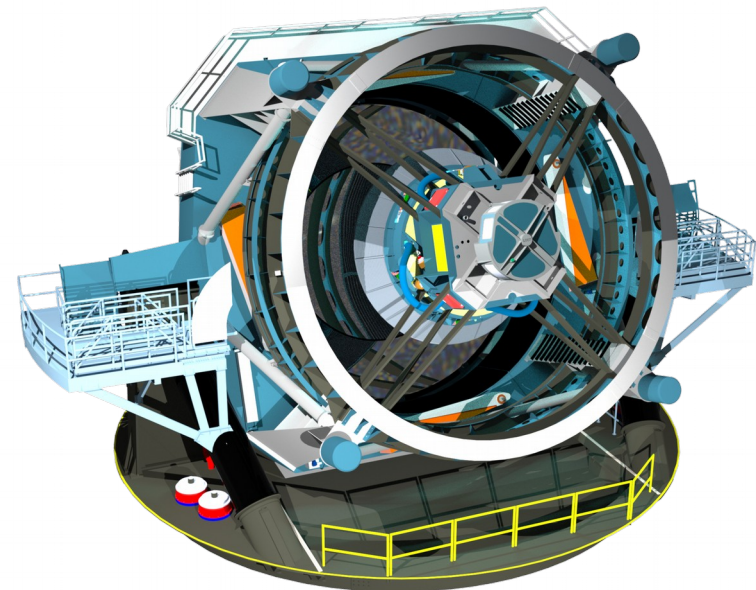
- Gravitational waves → properties of neutron stars (NSs) and high-density matter



Advanced LIGO

- Ejecta → rapid neutron-capture process (r-process) forging heavy elements such as gold

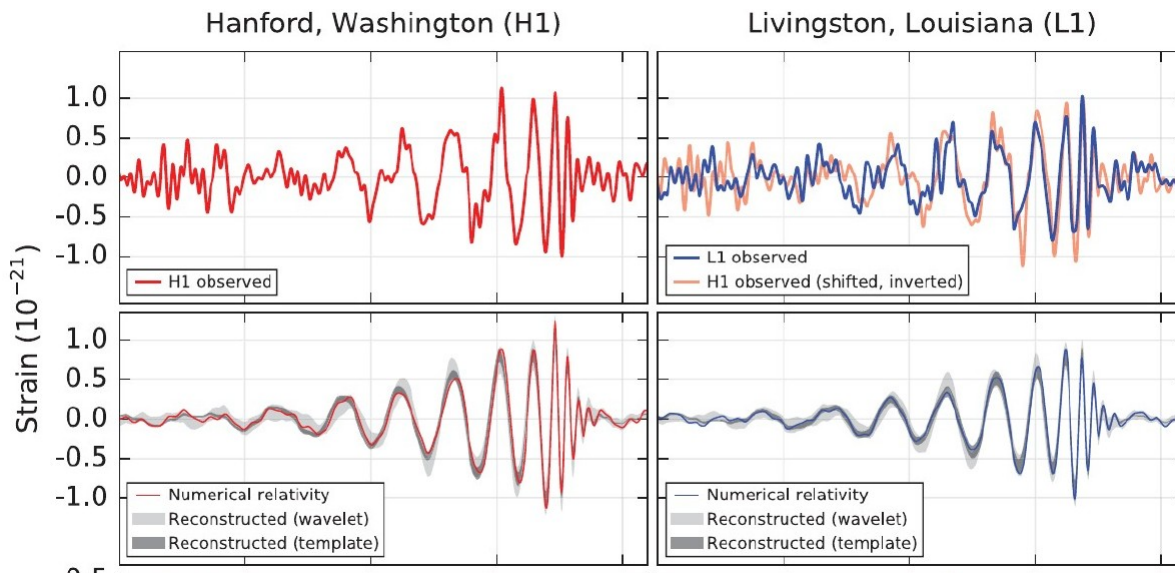
- Thermal emission → electromagnetic transient powered by radioactive decays in ejecta
- Accretion torus → Relativistic jet → short gamma-ray burst (frequently observed)



Large Synoptic Survey Telescope

Gravitational waves

- Recent detection of GWs from BH: breakthrough in astrophysics
- Fundamentally need way of observing astrophysical processes
- Next type of source to be detected: NS mergers !!!
- Scientific potential: rates, population properties, masses, ...
- Properties of nuclear matter – Neutron-star properties unknown
 - Details of GW signal constrain EoS / NS properties



Advanced LIGO

Formation of heavy elements and em transients

- **Astrophysical origin of heavy elements** formed through the rapid neutron-capture process is unknown – examples: gold, uranium, ...
- NS mergers provide favorable conditions for the r-process
- Numerous astronomical observations, Galactic enrichment
- Nuclear decays during r-process heat ejecta → thermal emission
- **Electromagnetic counterpart** potentially observable with optical survey telescopes → GW searches become more sensitive, details of nucleosynthesis
- (mergers are likely the origin of short gamma-ray bursts !!!)

Outline

- Neutron stars (in binaries)
- Merger rates
- Inspiral dynamics and GW observations
- EoS constraints from the inspiral phase
- EoS constraints from the postmerger phase
- Classification of postmerger dynamics/ GWs

See also Michal's talk !

Neutron stars

- NSs are formed in **core-collapse supernovae** of massive stars ($> 8 M_{\text{sun}}$)
- Masses between $\sim 1 \dots \sim 2 M_{\text{sun}}$ - upper limit depends on unknown EoS, but for sure $> 2 M_{\text{sun}}$ (observations in Demorest et al 2010, Antoniadis et al. 2010)
- Observable in radio, IR, optical, UV, X-rays, gamma
- Many NSs (~ 2000) are observed as **pulsars** (very regular radio emission) \rightarrow **rotation periods seconds to milliseconds**
- **Some are found in binary systems**
- Stellar structure solely determined by **high-density matter EoS**, in particular mass-radius relation (typical radii $\sim 10\text{-}15$ km)
- **EoS not known – stellar structure not known** (\rightarrow we rely on theoretical prescriptions of high-density matter)

Recall: stellar structure given by Tolman-Oppenheimer-Volkoff eqs.

For nonrotating NSs (or sufficiently slow rotation)

Stellar structure and thus M-R relation fully determined by EoS $P(\epsilon)$

$$\frac{dM}{dr} = 4\pi r^2 \epsilon$$

$$\frac{dP}{dr} = -\frac{GM\epsilon}{r^2} \left(1 + \frac{P}{\epsilon c^2}\right) \left(1 + \frac{4\pi r^3 P}{Mc^2}\right) \left(1 - \frac{2GM}{c^2 r}\right)^{-1}$$

Coupled system of ODEs – integrate outwards starting with given central density/pressure until $P=0 \rightarrow r(P=0)=R$

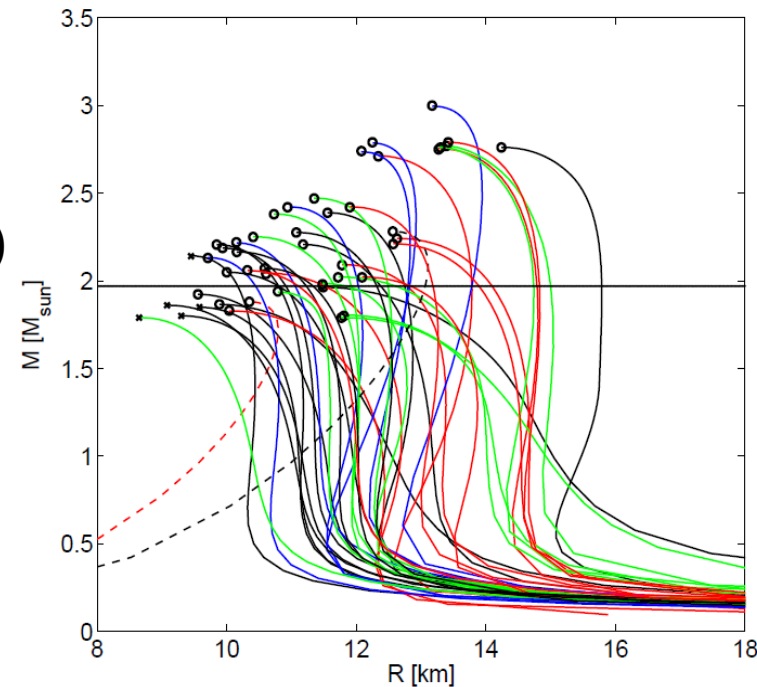
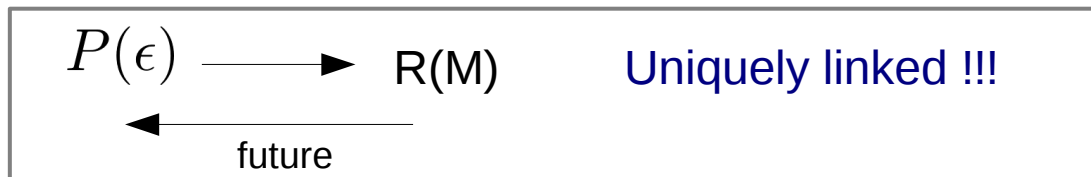
$M(R) = M$

M: gravitational mass $< M_0$ rest mass (baryonic mass)

R: circumferential radius

Integrate starting from different central densities

$\rightarrow M(\rho_0), R(\rho_0)$



Neutron stars in binaries

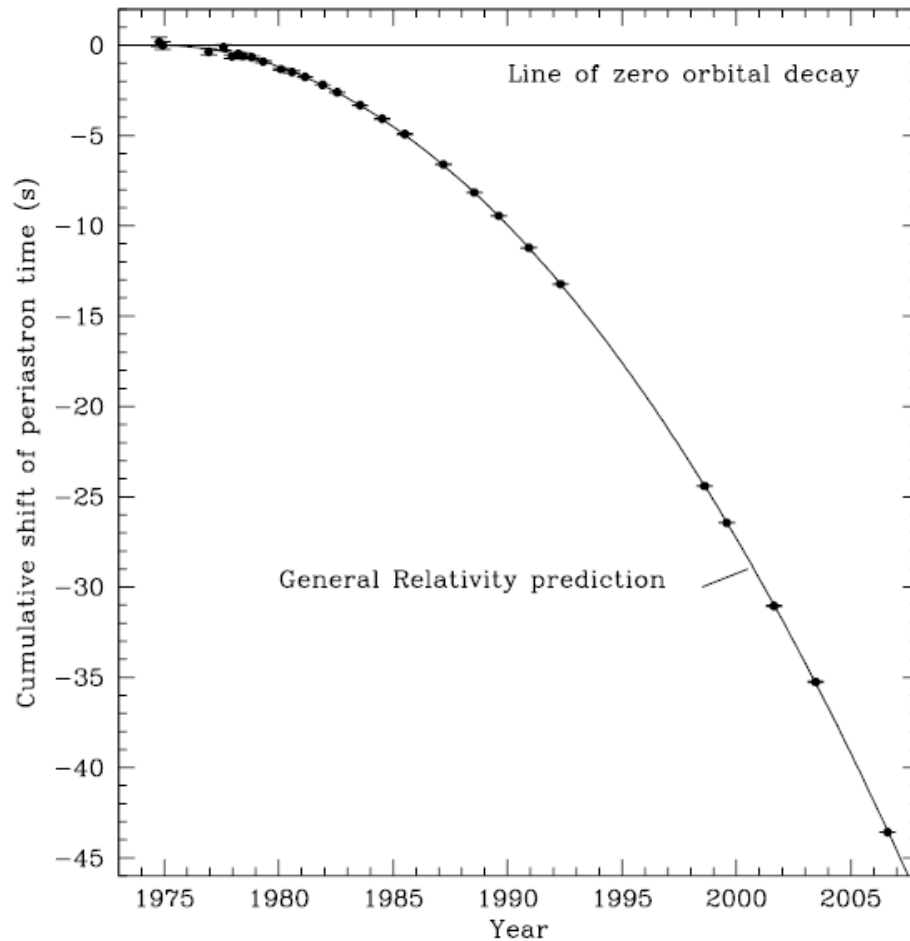
Neutron stars in binaries

<i>neutron star – neutron star binaries (mean $1.322 M_{\odot}$, error-weighted mean $1.402 M_{\odot}$)</i>					
J1829+2456 [‡]	$1.25^{+0.11}_{-0.35}$	z (42)	Companion	$1.34^{+0.37}_{-0.10}$	z (42)
J1811-1736 [‡]	$1.53^{+0.22}_{-0.63}$	A (43)	Companion	$1.04^{+0.73}_{-0.12}$	A (43)
J1906+0746	$1.248^{+0.018}_{-0.018}$	B (44)	Companion	$1.365^{+0.018}_{-0.018}$	B (44)
J1518+4904	$1.23^{+0.00}_{-0.33}$	C (27)	Companion	$1.49^{+0.33}_{-0.00}$	C (27)
B1534+12	$1.3332^{+0.0010}_{-0.0010}$	K (45)	Companion	$1.3452^{+0.0010}_{-0.0010}$	K (45)
B1913+16	$1.4398^{+0.0002}_{-0.0002}$	q (46)	Companion	$1.3886^{+0.0002}_{-0.0002}$	q (46)
B2127+11C♣	$1.358^{+0.010}_{-0.010}$	x (47)	Companion♣	$1.354^{+0.010}_{-0.010}$	x (47)
J0737-3039A	$1.3381^{+0.0007}_{-0.0007}$	i (48)	J0737-3039B	$1.2489^{+0.0007}_{-0.0007}$	i (48)
J1756-2251	$1.312^{+0.017}_{-0.017}$	J (49)	Companion	$1.258^{+0.017}_{-0.017}$	J (49)
J1807-2500B♣	$1.3655^{+0.0020}_{-0.0020}$	s (29)	Companion ?	$1.2064^{+0.0020}_{-0.0020}$	s (29)

- About 10 NS-NS systems known (at least one star being a pulsar) Lattimer 2012
- Some masses very accurately measured
- Systems are fairly symmetric, masses cluster around 1.3 - 1.4 Msun
- But Low number statistics – nobody can exclude bias
- Also other types of binaries including one NS are known, e.g. with white dwarf companion
- But no NS-black hole binary known yet

Why do NSs merge?

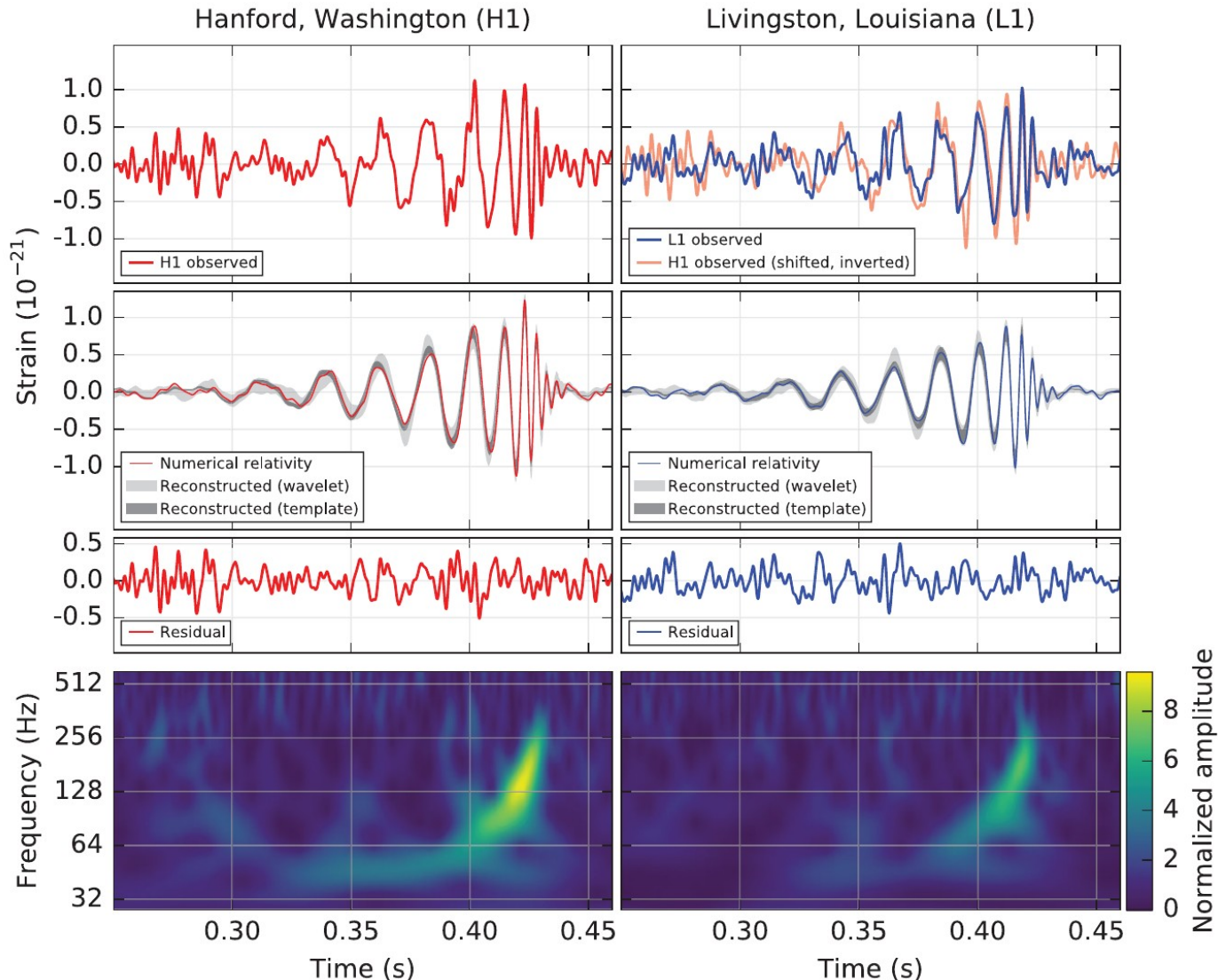
- Gravitational waves: $L_{GW} = -\frac{dE_{binary}}{dt}$



→ indirect evidence for the existence of GWs

Weisberg et al. 2010

Completely equivalent to the observed merger of two black holes



First direct observation of [gravitational waves](#)
by Advanced Ligo network - Autumn 2015

Abbott et al 2016

GWs lead to inspiral

- Orbital motion generates GWs, which carry away energy !!
- energy is extracted from orbit → decay of the orbit
- Assuming orbiting point particles with orbital separation a (Kepler's law - Newtonian):

$$L_{GW} = \frac{32 G^4 M^3 \mu^2}{5 c^5 a^5} \quad \Omega^2 = \frac{GM}{a^3}$$

with $M := M_1 + M_2$ $\mu := \frac{M_1 M_2}{M}$

Decay of the orbit: $\dot{a} = -\frac{64 G^3 \mu M^2}{5 c^5 a^3}$ Increase of orb. frequency !

Integrate → merger time: $\tau = \frac{5 c^5 a_0^4}{256 G^3 \mu M^4}$ For circular orbits

Observed systems

	J0737–3039	J1518+4904	B1534+12	J1756–2251	J1811–1736
P [ms]	22.7/2770	40.9	37.9	28.5	104.2
P_b [d]	0.102	8.6	0.4	0.32	18.8
e	0.088	0.25	0.27	0.18	0.83
$\log_{10}(\tau_c/[yr])$	8.3/7.7	10.3	8.4	8.6	9.0
$\log_{10}(\tau_g/[yr])$	7.9	12.4	9.4	10.2	13.0
Masses measured?	Yes	No	Yes	Yes	Yes
	B1820–11	J1829+2456	J1906+0746	B1913+16	B2127+11C
P [ms]	279.8	41.0	144.1	59.0	30.5
P_b [d]	357.8	1.18	0.17	0.3	0.3
e	0.79	0.14	0.085	0.62	0.68
$\log_{10}(\tau_c/[yr])$	6.5	10.1	5.1	8.0	8.0
$\log_{10}(\tau_g/[yr])$	15.8	10.8	8.5	8.5	8.3
Masses measured?	No	No	Yes	Yes	Yes

Lorimer 2008

- Typical **orbital period: hours !** (→ current emission too weak / frequency outside sensitivity window of ground-based detectors)
- Typical (intrinsic) rotation period: 100 ms (of pulsar), (relatively slow)
- Typical time until merging = **inspiral time: 100 Myrs** (or much longer)
- Hubble time: $\sim 10^{10}$ yrs
 → **NS binaries may merge** (again: low number statistics; rate estimate difficult - later)

Formation of NS binaries

Standard evolutionary channel: (variations possible, many things still unclear)

- **Binary of massive stars** (both $> 8 M_{\text{sun}}$), recall many stars in binaries
- More massive component explodes as SN after a few millions (recall more massive stars evolve faster)
- Secondary evolves and fills Roche lobe \rightarrow mass overflow
- NS moves in **common envelope** (dynamical friction) \rightarrow reduction of orbital separation (crucial for small orbital separations and thus merging), energy deposition in envelope
- Secondary explodes as supernova

Complications: star formation, binary formation, kicks by explosions, common-envelope phase hard to model, outcome of explosion (NS vs. BH), ..., possibly other formation channels: CE before first explosion, dynamical captures in star clusters, ...

Estimated rates

TABLE VI: Estimates of NS-NS inspiral rates.

Rate model	R_{low}		R_{re}		R_{high}		R_{max}	
	MWEG ⁻¹	Myr ⁻¹	MWEG ⁻¹	Myr ⁻¹	MWEG ⁻¹	Myr ⁻¹	MWEG ⁻¹	Myr ⁻¹
Extrapolation: Model 6 of Kim et al. [33] ^a	16.9		83.0		292.1			
Extrapolation: Model 14 of Kim et al. [33] ^a	1.0		3.8		13.2			
Extrapolation: Model 15 of Kim et al. [33] ^a	43.1		223.7		817.5			
O’Shaughnessy et al. pop. synth. [18] ^b	5		30		300			
Voss & Tauris pop. synth. [34] ^c	0.54		1.5		17			
Belczynski et al. pop. synth.: model A of [35] ^d			12					
Belczynski et al. pop. synth.: model B of [35] ^d			7.6					
Belczynski et al. pop. synth.: model C of [35] ^d			68					
Nelemans pop. synth. [36] ^e	0.5		25		1250			
“Double-core” scenario: Dewi et al. [37] ^f	0.91		12.10					
With ellipticals: de Freitas Pacheco et al. [23] ^g			34					
Supernova Ib/Ic limit [16] ^h								3900

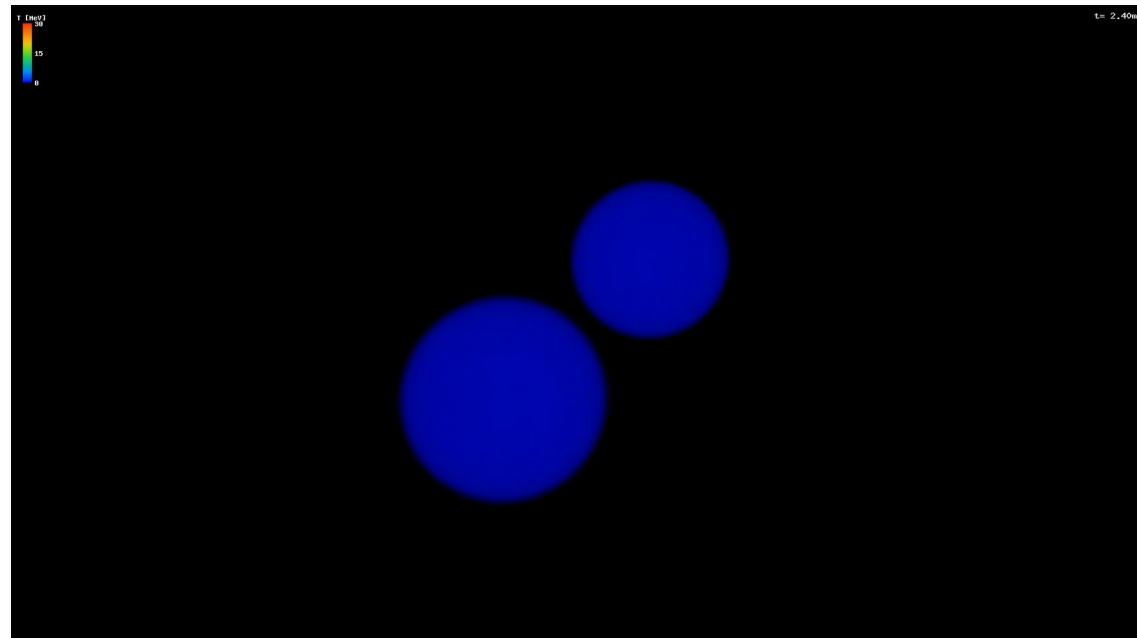
Abadie et al. 2010

(Most) computed via population synthesis modeling all effects in some way

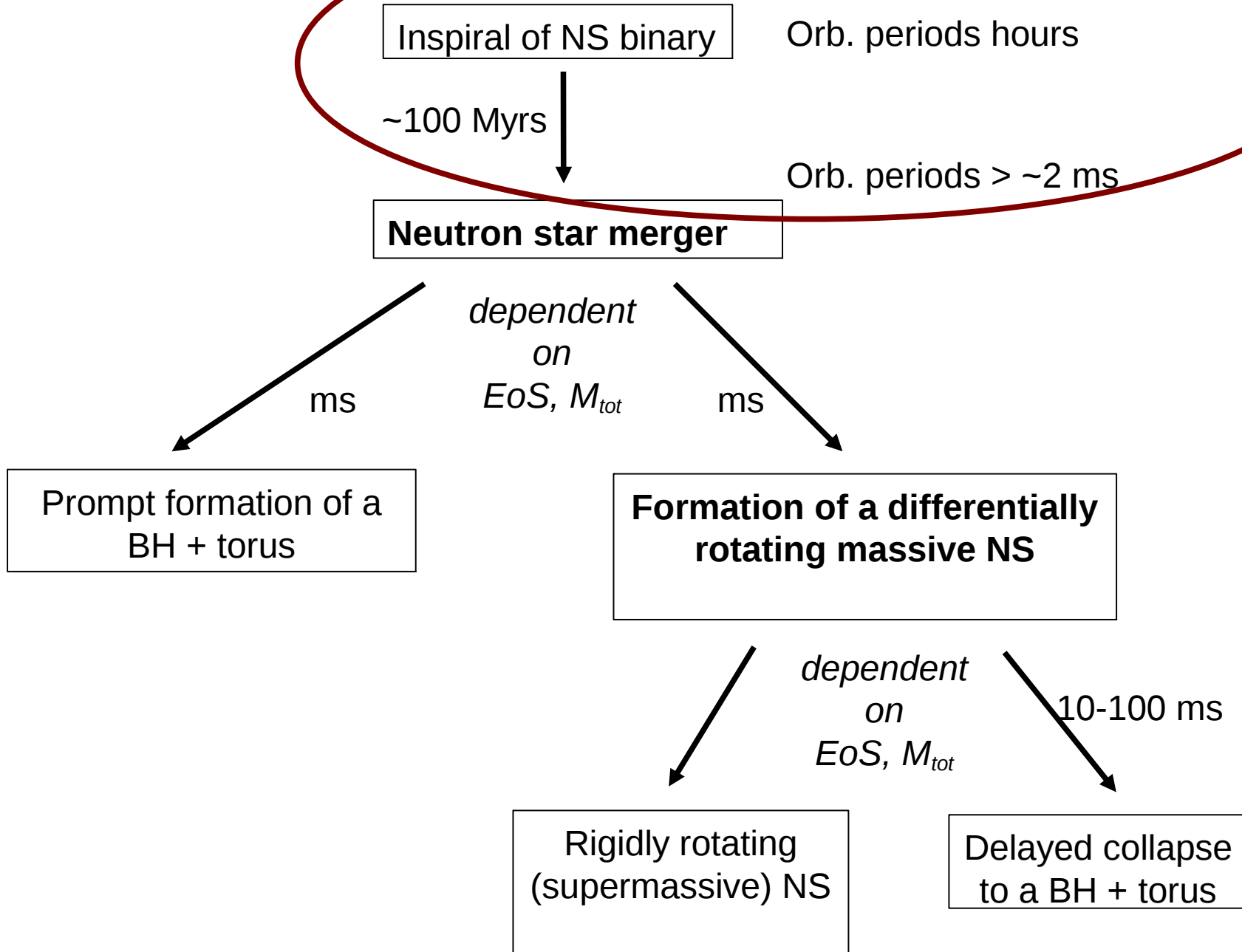
NS merger rate only roughly known: ~ 10 ... 100 events per Myr in our Galaxy → ~ 40 detections with Ad. LIGO/Virgo

Alternative estimates: observed population of NS binaries, rate of short gamma-ray bursts, nucleosynthesis → all roughly agree on the order of magnitude !!

Overview merger stages



Dynamics



Inspiral dynamics

Ingredients: Newtonian point-particle dynamics + Quadrupole formula

$$L_{GW} = -\frac{dE_{binary}}{dt}$$

Sufficient for most of the inspiral phase except for last cycles (later)

$$\Omega^2 = \frac{GM}{a^3} \quad \Omega_{GW} = 2\Omega$$

Define **chirp mass**: $\mathcal{M} := \mu^{3/5} M^{2/5}$

With total mass M
and reduced mass μ

GW amplitude:
$$\bar{h}_{xx}^{TT} = -2^{1/3} \frac{\mathcal{M}^{5/3} \Omega_{GW}^{2/3}}{r} \cos[\Omega_{GW}(t - r)]$$

For given instantaneous GW / orbital frequency

Inspiral dynamics

Ingredients: Newtonian point-particle dynamics + Quadrupole formula

$$L_{GW} = -\frac{dE_{binary}}{dt}$$

Sufficient for the most of inspiral phase except for last cycles (later)

$$\Omega^2 = \frac{GM}{a^3} \qquad \Omega_{GW} = 2\Omega$$

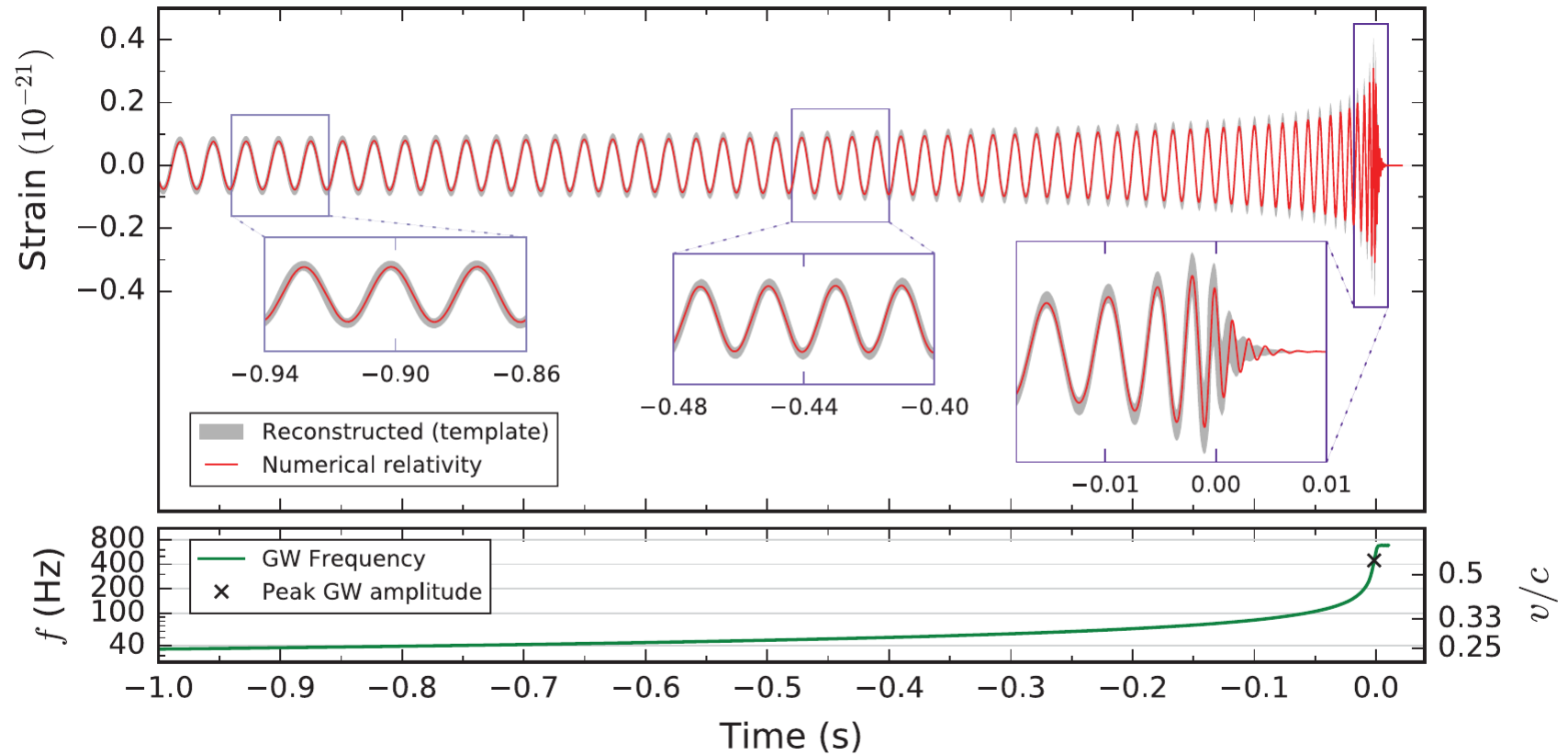
Frequency / orbital evolution:

$$\dot{a} = -\frac{64}{5} \frac{G^3}{c^5} \frac{\mu M^2}{a^3} \quad \Leftrightarrow \quad \dot{\Omega}_{GW} = \frac{12 \times 2^{1/3}}{5} \mathcal{M}^{5/3} \Omega_{GW}^{11/3}$$

Chirp mass determines amplitude and frequency evolution !!!

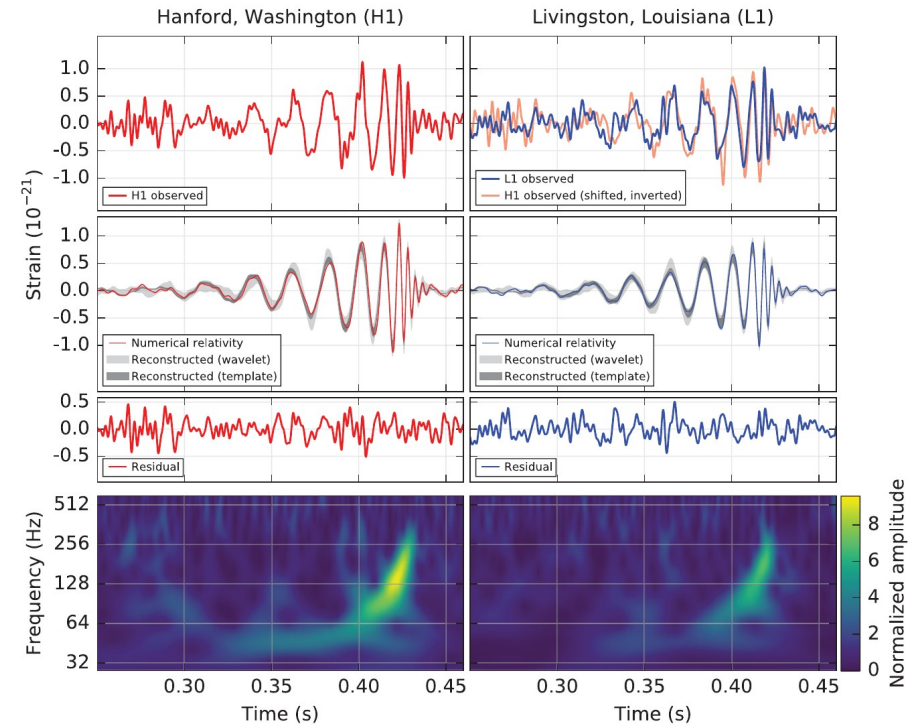
=> primary parameter to be measured in GW detection

As for BH merger



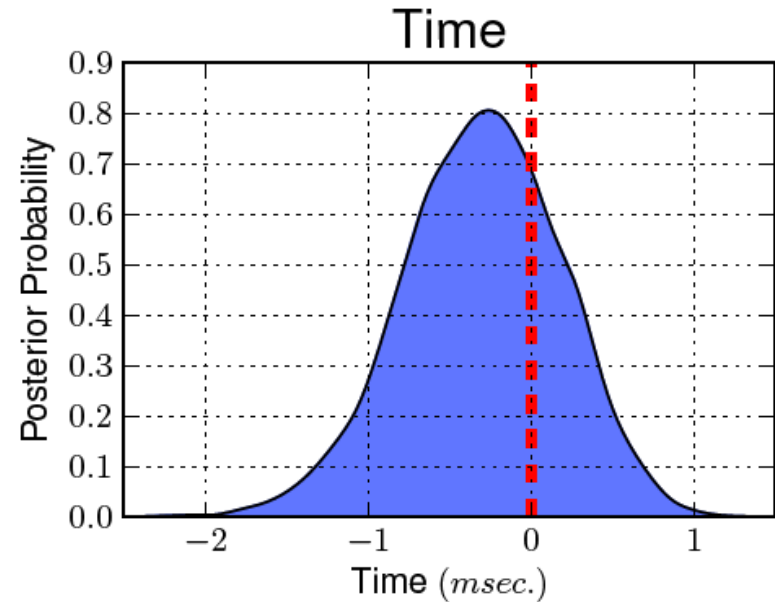
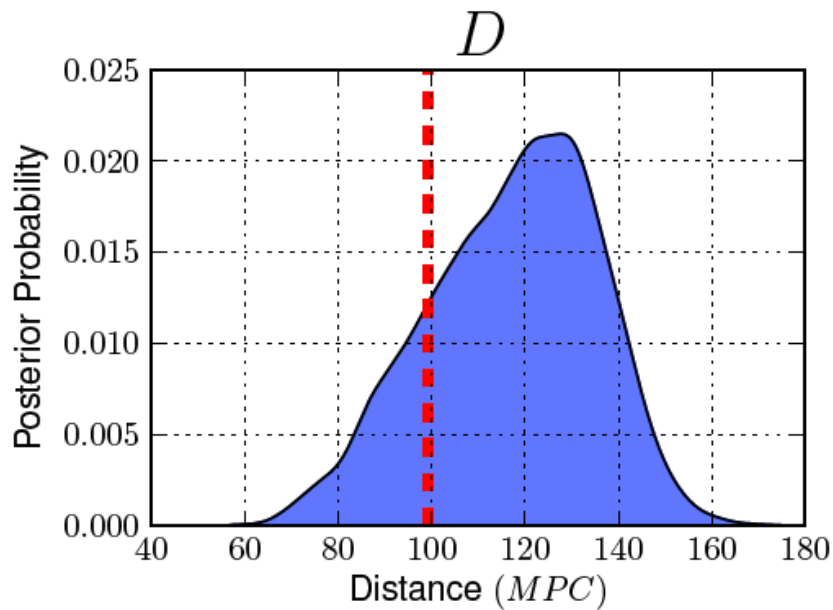
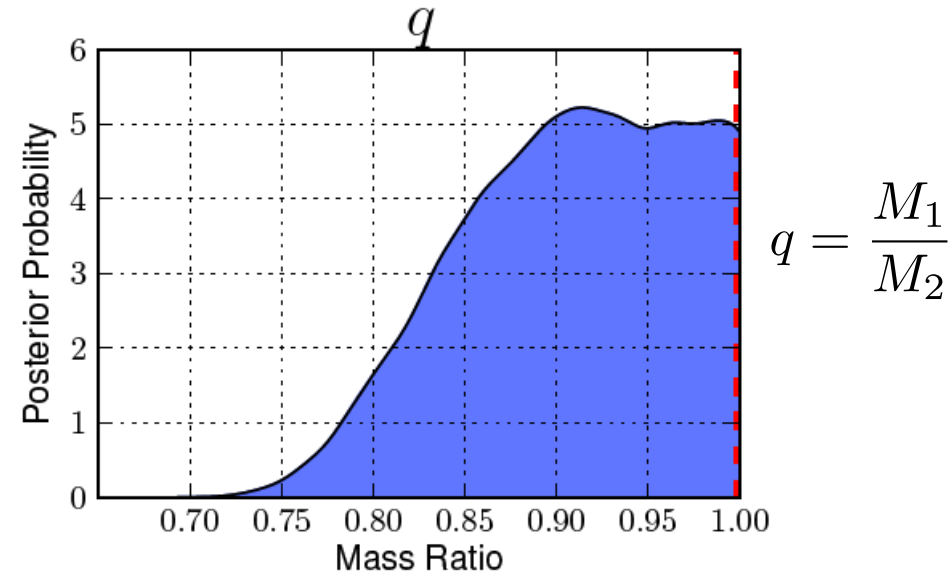
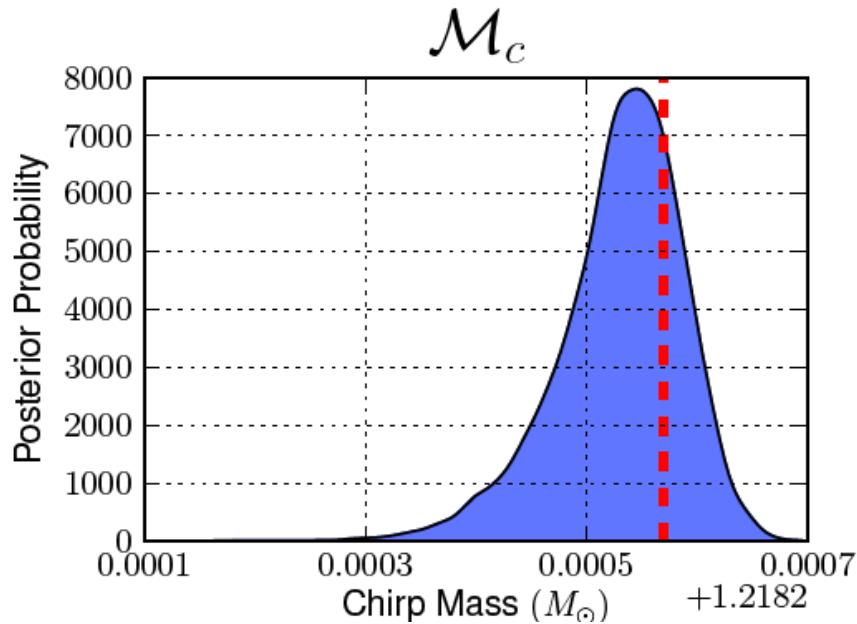
- Equivalent for BH mergers - and in fact already measured !!!!

Event	GW150914	GW151226	LVT151012
Signal-to-noise ratio ρ	23.7	13.0	9.7
False alarm rate FAR/yr ⁻¹	$< 6.0 \times 10^{-7}$	$< 6.0 \times 10^{-7}$	0.37
p-value	7.5×10^{-8}	7.5×10^{-8}	0.045
Significance	$> 5.3 \sigma$	$> 5.3 \sigma$	1.7σ
Primary mass m_1/M_\odot	$36.2^{+5.2}_{-3.8}$	$14.2^{+8.3}_{-3.7}$	23^{+18}_{-6}
Secondary mass m_2/M_\odot	$29.1^{+3.7}_{-4.4}$	$7.5^{+2.3}_{-2.3}$	13^{+4}_{-5}
Chirp mass $M_{\text{source}}/M_\odot$	$28.1^{+1.8}_{-1.5}$	$8.9^{+0.3}_{-0.3}$	$15.1^{+1.4}_{-1.1}$
Total mass $M_{\text{source}}/M_\odot$	$65.3^{+4.1}_{-3.4}$	$21.8^{+5.9}_{-1.7}$	37^{+13}_{-4}
Effective inspiral spin χ_{eff}	$-0.06^{+0.14}_{-0.14}$	$0.21^{+0.20}_{-0.10}$	$0.0^{+0.3}_{-0.2}$
Final mass M_f/M_\odot	$62.3^{+3.7}_{-3.1}$	$20.8^{+6.1}_{-1.7}$	35^{+14}_{-4}
Final spin a_f	$0.68^{+0.05}_{-0.06}$	$0.74^{+0.06}_{-0.06}$	$0.66^{+0.09}_{-0.10}$
Radiated energy $E_{\text{rad}}/(M_\odot c^2)$	$3.0^{+0.5}_{-0.4}$	$1.0^{+0.1}_{-0.2}$	$1.5^{+0.3}_{-0.4}$
Peak luminosity $\ell_{\text{peak}}/(\text{erg s}^{-1})$	$3.6^{+0.5}_{-0.4} \times 10^{56}$	$3.3^{+0.8}_{-1.6} \times 10^{56}$	$3.1^{+0.8}_{-1.8} \times 10^{56}$
Luminosity distance D_L/Mpc	420^{+150}_{-180}	440^{+180}_{-190}	1000^{+500}_{-500}
Source redshift z	$0.09^{+0.03}_{-0.04}$	$0.09^{+0.03}_{-0.04}$	$0.20^{+0.09}_{-0.09}$
Sky localization $\Delta\Omega/\text{deg}^2$	230	850	1600



What can we learn from the inspiral?

What can we learn from inspiral I



Posterior Probability Densities for $1.4M_\odot/1.4M_\odot$ System

Rodriguez et al 2014

Note: mass ratio, spins, ... enter only at higher post-Newtonian order \rightarrow harder to measure

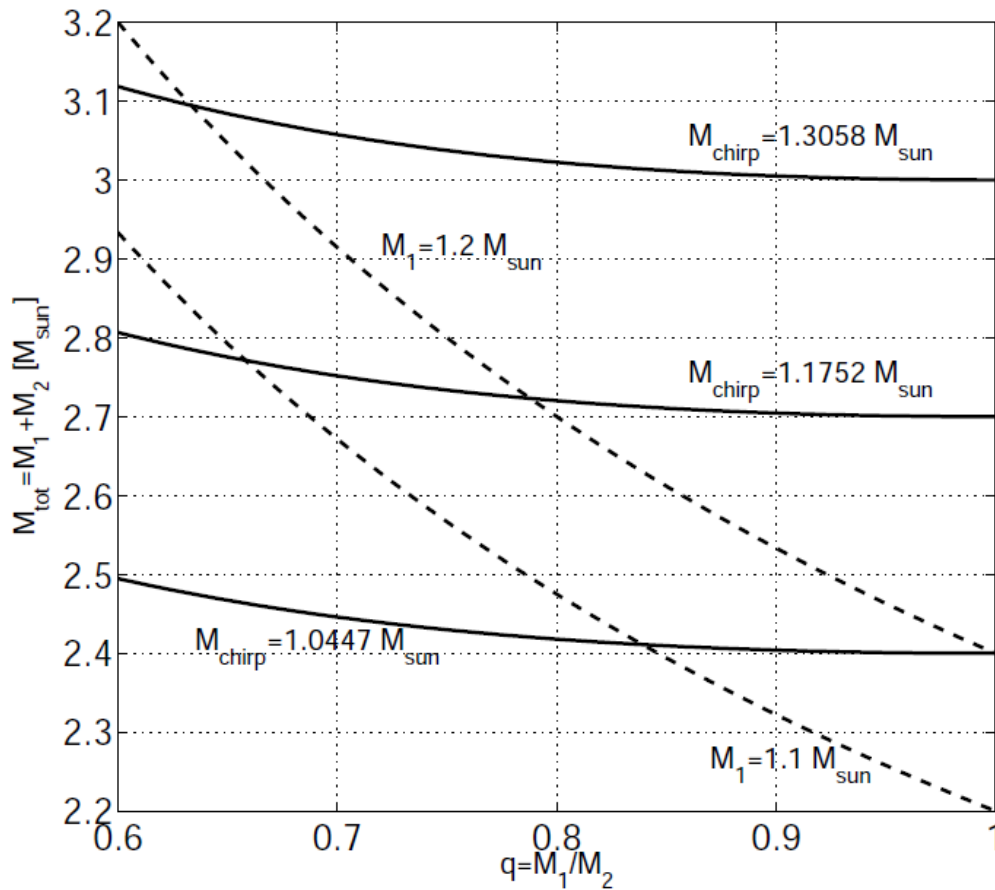
- Equivalent for BH mergers

Event	GW150914	GW151226	LVT151012
Signal-to-noise ratio ρ	23.7	13.0	9.7
False alarm rate FAR/yr ⁻¹	$< 6.0 \times 10^{-7}$	$< 6.0 \times 10^{-7}$	0.37
p-value	7.5×10^{-8}	7.5×10^{-8}	0.045
Significance	$> 5.3 \sigma$	$> 5.3 \sigma$	1.7σ
Primary mass $m_1^{\text{source}}/M_\odot$	$36.2^{+5.2}_{-3.8}$	$14.2^{+8.3}_{-3.7}$	23^{+18}_{-6}
Secondary mass $m_2^{\text{source}}/M_\odot$	$29.1^{+3.7}_{-4.4}$	$7.5^{+2.3}_{-2.3}$	13^{+4}_{-5}
Chirp mass $\mathcal{M}^{\text{source}}/M_\odot$	$28.1^{+1.8}_{-1.5}$	$8.9^{+0.3}_{-0.3}$	$15.1^{+1.4}_{-1.1}$
Total mass $M^{\text{source}}/M_\odot$	$65.3^{+4.1}_{-3.4}$	$21.8^{+5.9}_{-1.7}$	37^{+13}_{-4}
Effective inspiral spin χ_{eff}	$-0.06^{+0.14}_{-0.14}$	$0.21^{+0.20}_{-0.10}$	$0.0^{+0.3}_{-0.2}$
Final mass $M_f^{\text{source}}/M_\odot$	$62.3^{+3.7}_{-3.1}$	$20.8^{+6.1}_{-1.7}$	35^{+14}_{-4}
Final spin a_f	$0.68^{+0.05}_{-0.06}$	$0.74^{+0.06}_{-0.06}$	$0.66^{+0.09}_{-0.10}$
Radiated energy $E_{\text{rad}}/(M_\odot c^2)$	$3.0^{+0.5}_{-0.4}$	$1.0^{+0.1}_{-0.2}$	$1.5^{+0.3}_{-0.4}$
Peak luminosity $\ell_{\text{peak}}/(\text{erg s}^{-1})$	$3.6^{+0.5}_{-0.4} \times 10^{56}$	$3.3^{+0.8}_{-1.6} \times 10^{56}$	$3.1^{+0.8}_{-1.8} \times 10^{56}$
Luminosity distance D_L/Mpc	420^{+150}_{-180}	440^{+180}_{-190}	1000^{+500}_{-500}
Source redshift z	$0.09^{+0.03}_{-0.04}$	$0.09^{+0.03}_{-0.04}$	$0.20^{+0.09}_{-0.09}$
Sky localization $\Delta\Omega/\text{deg}^2$	230	850	1600

What we learn from the chirp mass?

Chirp mass practically precisely measured

under assumption that no information on intrinsic system parameters are available:



$$M_{\text{chirp}} = (M_1 M_2)^{3/5} (M_1 + M_2)^{-1/5}$$

$$M_{\text{tot}} = M_1 + M_2 \quad q = M_1/M_2$$

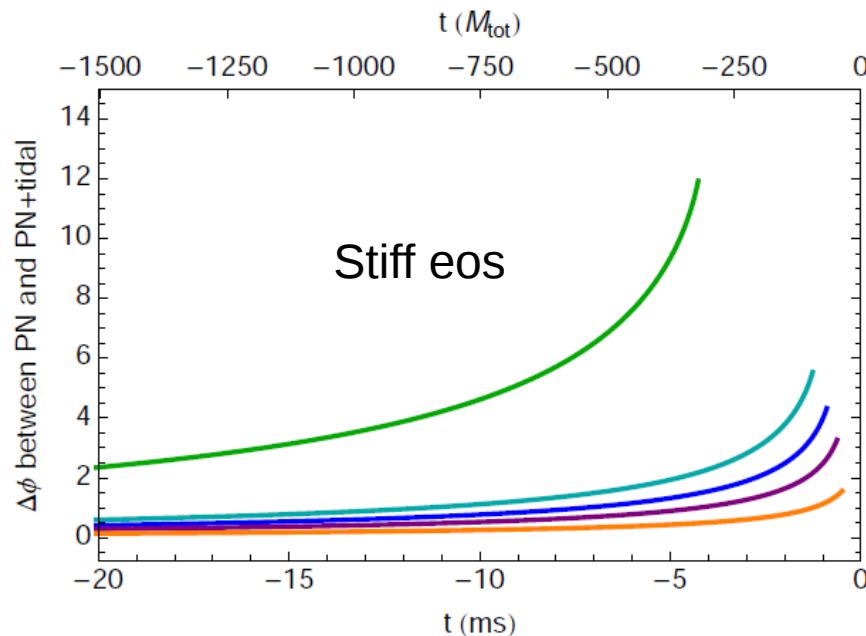
From core-collapse simulations: lowest NS mass $\sim 1.2 M_{\text{sun}}$ (e.g. Ertl et al. 2015)

\Rightarrow for typical mass range of NS-NS binaries ($2 * \sim 1.35 M_{\text{sun}}$):
total binary mass well measured

Inspiral and EoS constraints

What can we learn from the inspiral II

- Finite-size effects (**deviations from point-particle behavior**) enter the waveform at higher post-Newtonian order, e.g. play a role at higher orbital frequencies / in the very last cycles (evolution of phase)
- Description of these effects (within post-Newtonian theory, effective one-body descriptions guided by simulations) and construction of template bank active field of research



Read et al. 2013

→ distinguish EoSs !

Soft eos

FIG. 10. Top panel: The phase departures from point-particle Taylor-T4 due to post-Newtonian tidal contributions. From highest to lowest, the lines indicate EOS 2H, H, HB, B, and Bss. Bottom panel: The phase departures due to hybrid wave-

What can we learn from the inspiral II

- Waveforms incl. finite-size effects are described by **tidal deformability** (how a star reacts on an external tidal field)
- Offer possibility to constrain EoS because tidal deformability depends on EoS

$$\Lambda \equiv \frac{2}{3} k_2 \left(\frac{R}{M} \right)^5$$

- Corresponding to ~10 % error in radius R for nearby events (<100Mpc) (e.g. Read et al. 2013)
- Note: faithful templates to be constructed

R/M compactness (EoS dependent)

k_2 tidal love number (EoS dependent)

Computing the love number/tidal deformability

Extension of a standard TOV solver (i.e. numerically an integration of coupled ODEs):

Ansatz for the metric including a $l=2$ perturbation

$$\begin{aligned}
 ds^2 = & -e^{2\Phi(r)} [1 + H(r)Y_{20}(\theta, \varphi)] dt^2 \\
 & + e^{2\Lambda(r)} [1 - H(r)Y_{20}(\theta, \varphi)] dr^2 \\
 & + r^2 [1 - K(r)Y_{20}(\theta, \varphi)] (d\theta^2 + \sin^2 \theta d\varphi^2)
 \end{aligned}$$

Following Hinderer et al. 2010

Integrate standard TOV system:

And additional eqs. for perturbations:

$$\begin{aligned}
 e^{2\Lambda} &= \left(1 - \frac{2m_r}{r}\right)^{-1}, \\
 \frac{d\Phi}{dr} &= -\frac{1}{\epsilon + p} \frac{dp}{dr}, \\
 \frac{dp}{dr} &= -(\epsilon + p) \frac{m_r + 4\pi r^3 p}{r(r - 2m_r)}, \\
 \frac{dm_r}{dr} &= 4\pi r^2 \epsilon.
 \end{aligned}$$

$$\begin{aligned}
 \frac{dH}{dr} &= \beta \\
 \frac{d\beta}{dr} &= 2 \left(1 - 2\frac{m_r}{r}\right)^{-1} H \left\{ -2\pi [5\epsilon + 9p + f(\epsilon + p)] \right. \\
 &\quad \left. + \frac{3}{r^2} + 2 \left(1 - 2\frac{m_r}{r}\right)^{-1} \left(\frac{m_r}{r^2} + 4\pi r p\right)^2 \right\} \\
 &\quad + \frac{2\beta}{r} \left(1 - 2\frac{m_r}{r}\right)^{-1} \left\{ -1 + \frac{m_r}{r} + 2\pi r^2 (\epsilon - p) \right\}.
 \end{aligned} \tag{11}$$

EoS to be provided $\epsilon(p)$

($K(r)$ given by $H(r)$)

Note: Although multidimensional problem – computation in 1D since absorbed in Y_{20}

Computing the love number/tidal deformability

Numerical integration outwards until stellar surface $r=R$

Define compactness $C=M/R$ with $M=m(R)$ and $y = \frac{R\beta(R)}{H(R)}$

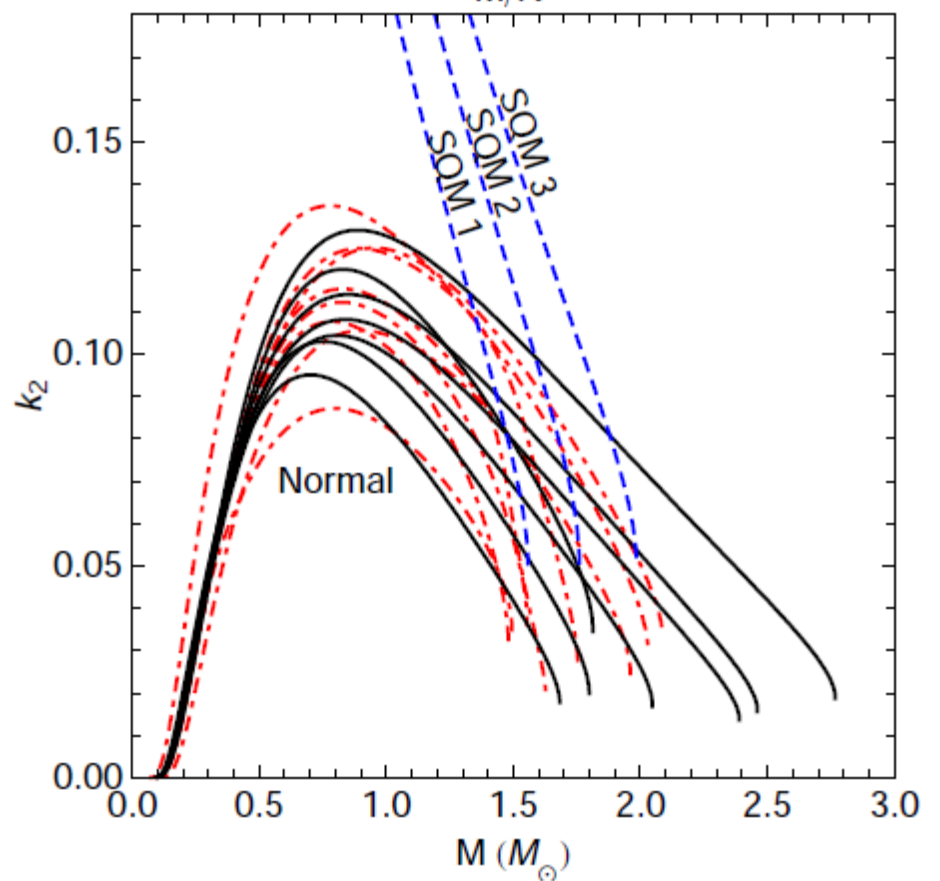
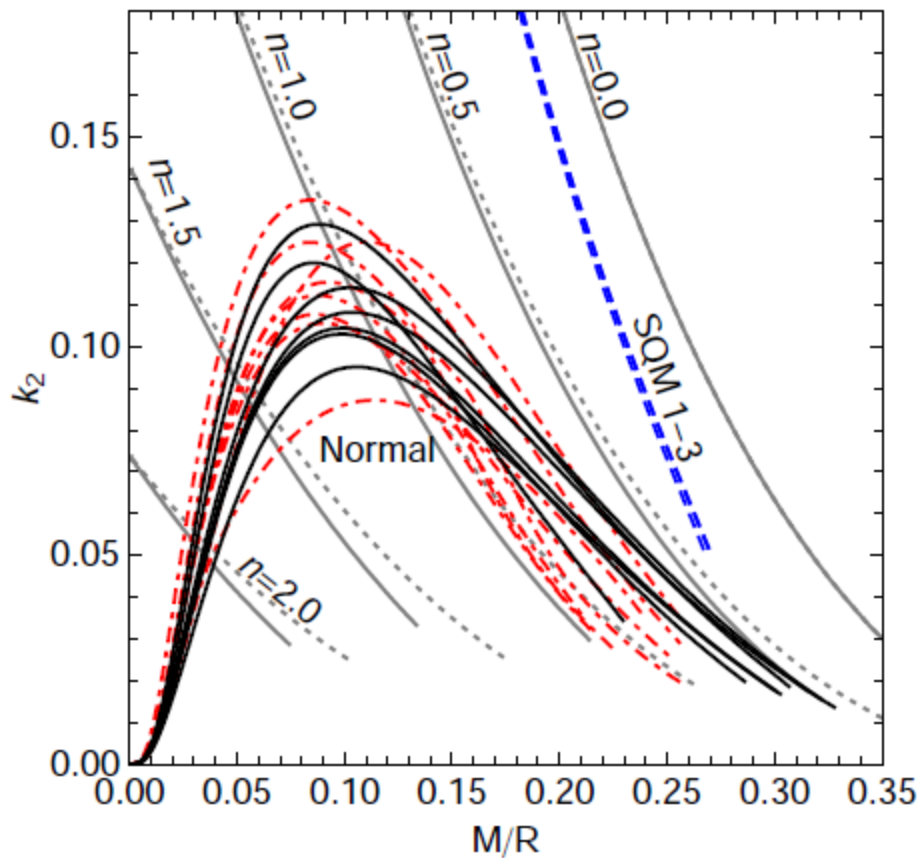
Love number is now given by (from comparison to asymptotic metric):

$$k_2 = \frac{8C^5}{5}(1-2C)^2[2+2C(y-1)-y] \\ \times \left\{ 2C[6-3y+3C(5y-8)] \right. \\ \left. + 4C^3[13-11y+C(3y-2)+2C^2(1+y)] \right. \\ \left. + 3(1-2C)^2[2-y+2C(y-1)]\ln(1-2C) \right\}^{-1}$$

=> Love number is a pure “TOV property”

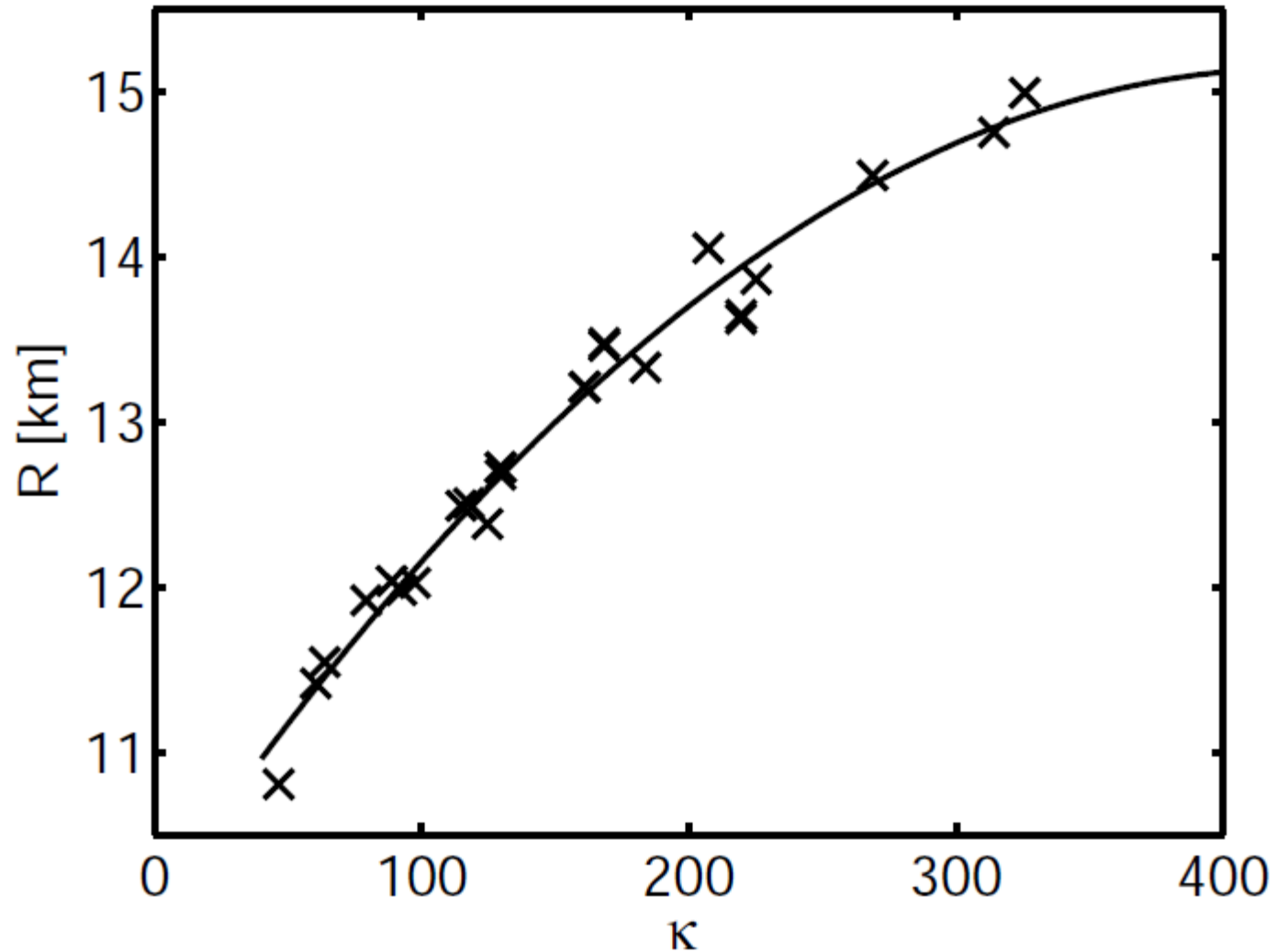
And can be obtained for a given EoS as function of central density or mass

Love number



For fixed compactness k_2 depends on EoS \Rightarrow tidal deformability is not a unique function of compactness for different EoSs

Tidal deformability vs radius

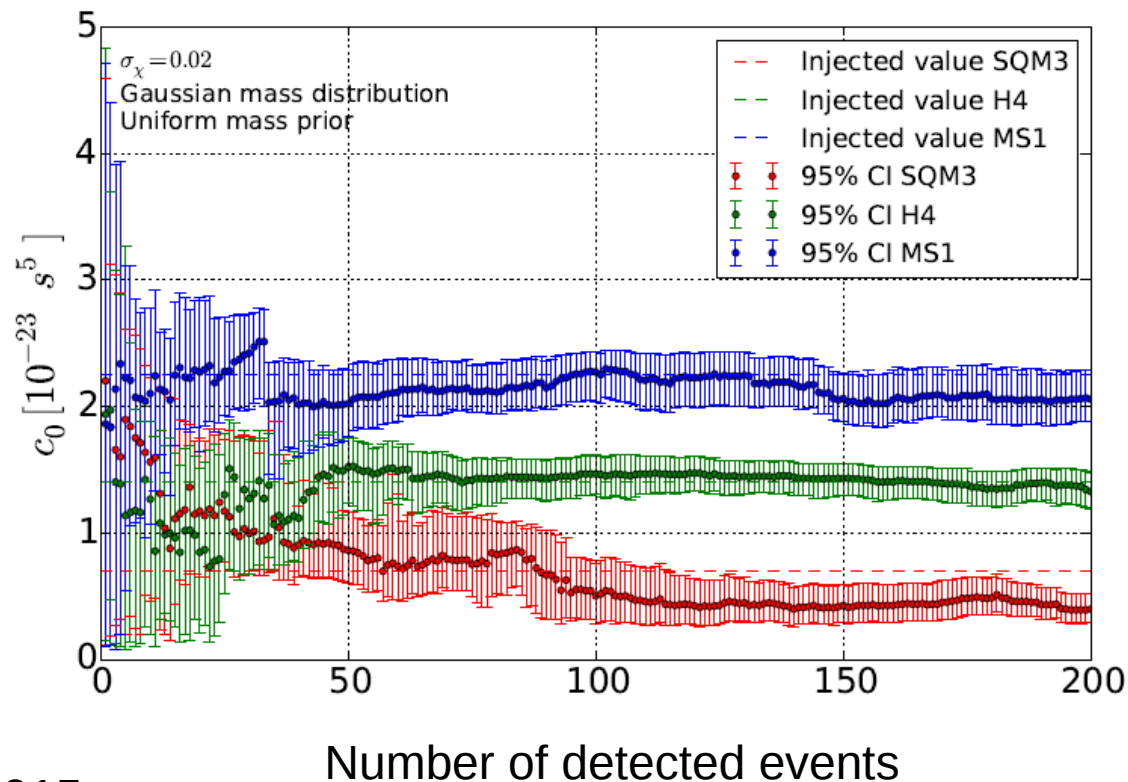


1.35 Msun stars with many different EoS, Bauswein 2015 unpublished, max dev. 314 meters

Tidal deformability

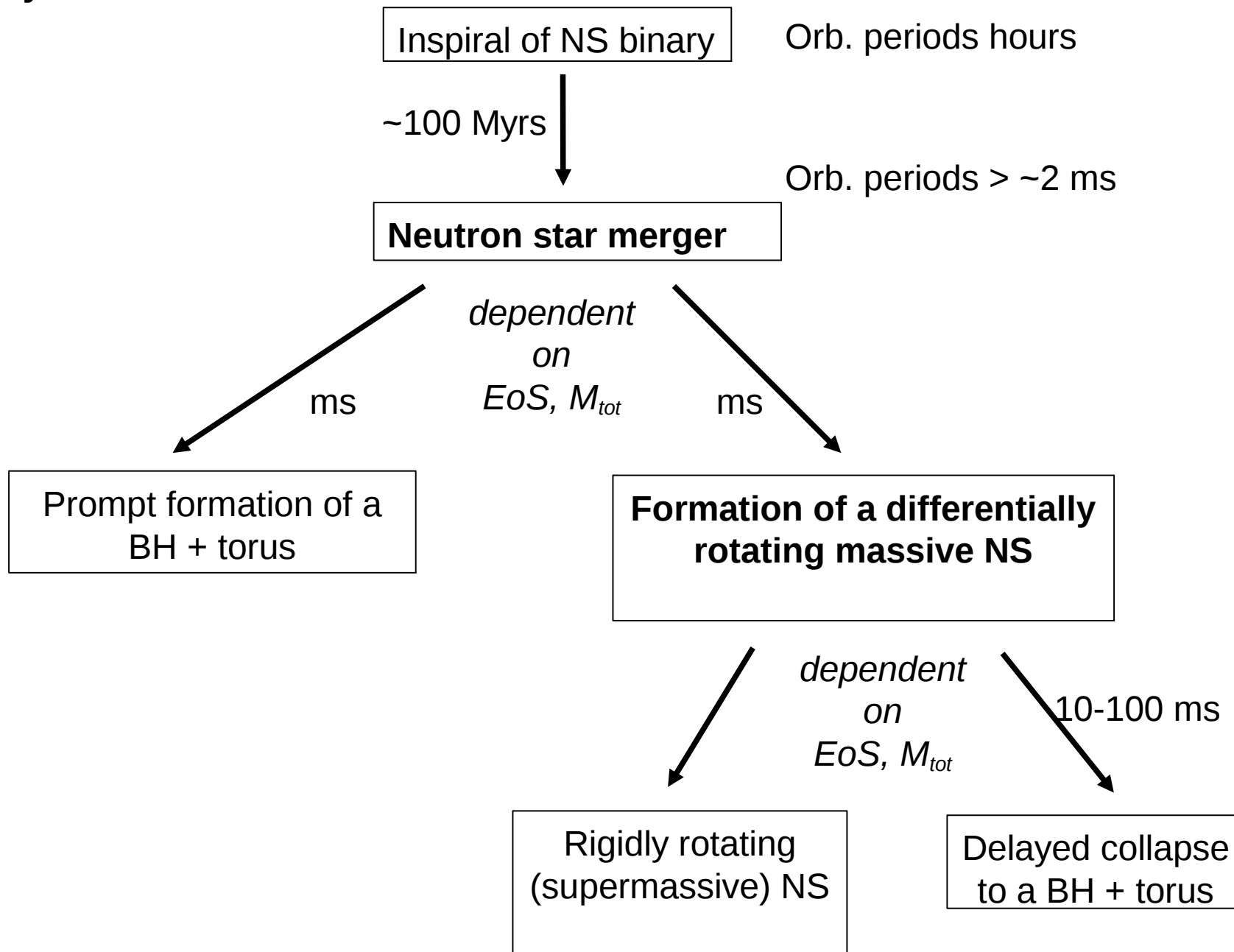
- Combining many detections at different distances / SNRs, astrophysically realistic random distribution of sources
- Note systematic errors on top of statistical error
- Many events allow to roughly discern EoSs

$$\lambda(m) = (2/3)k_2(m)R^5(m)$$

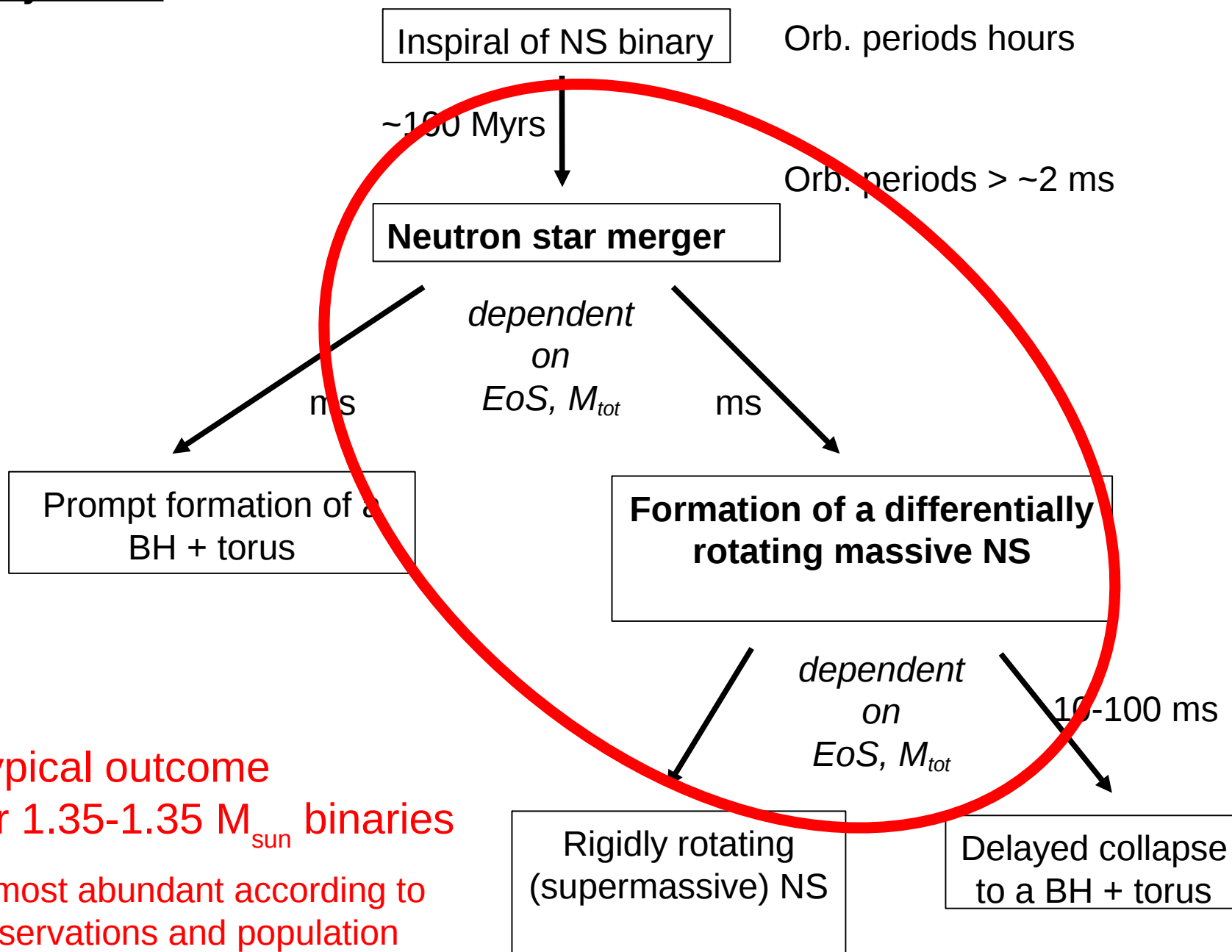


EoS constraints from postmerger phase
(discussion based in hydro-simulation results)

Dynamics



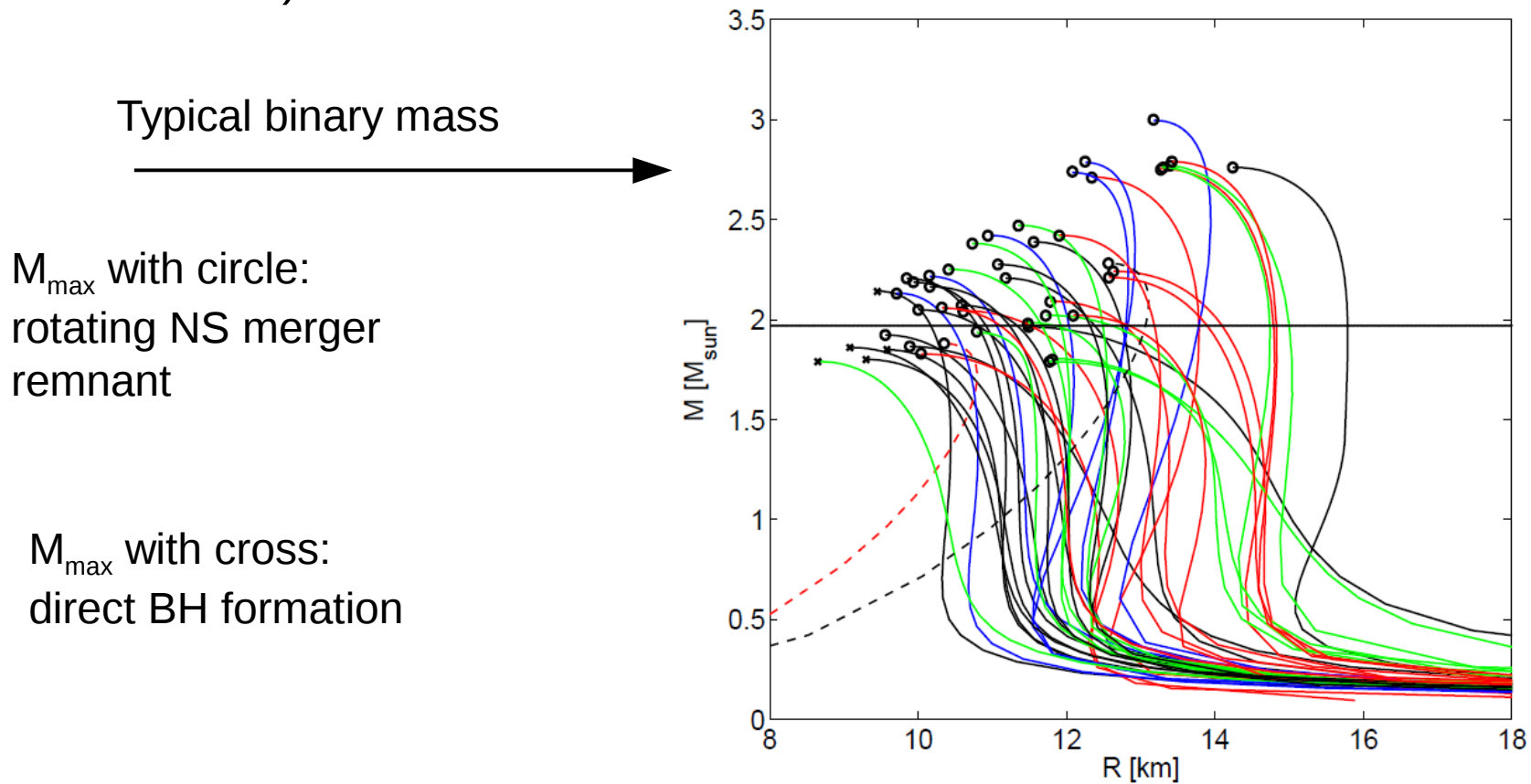
Dynamics



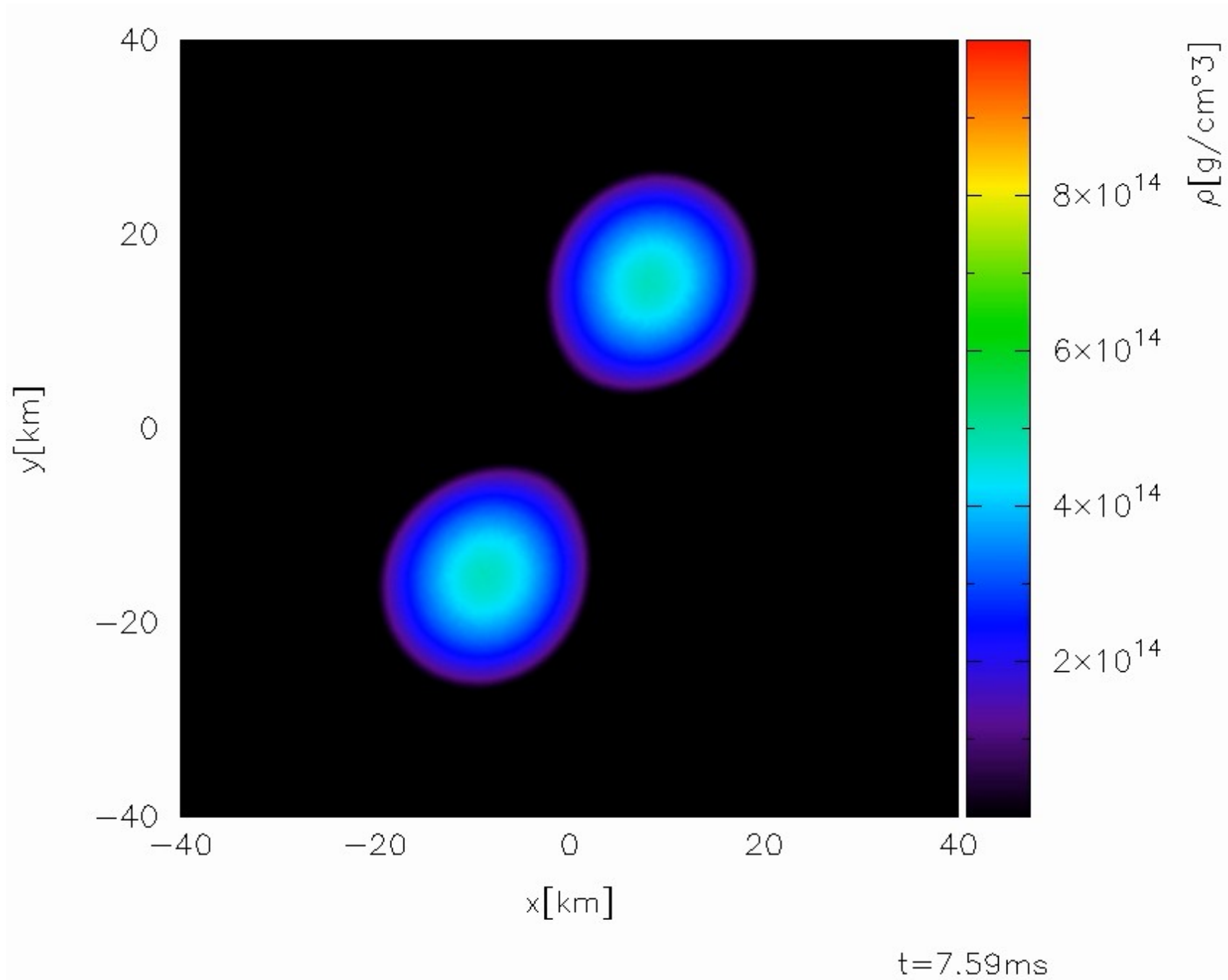
Typical outcome
for $1.35-1.35 M_{\text{sun}}$ binaries

(~most abundant according to
observations and population
synthesis)

- We should focus on 1.35-1.35 Msun systems (most common)
- Investigating different EoSs (affecting the outcome)
- Typical outcome: **hot, massive, differentially rotating NS merger remnant**
- Even if $M_{\text{tot, binary}} > M_{\text{max}}$ or max. mass of uniformly rotating NS ($\sim 1.2 \cdot M_{\text{max}}$)

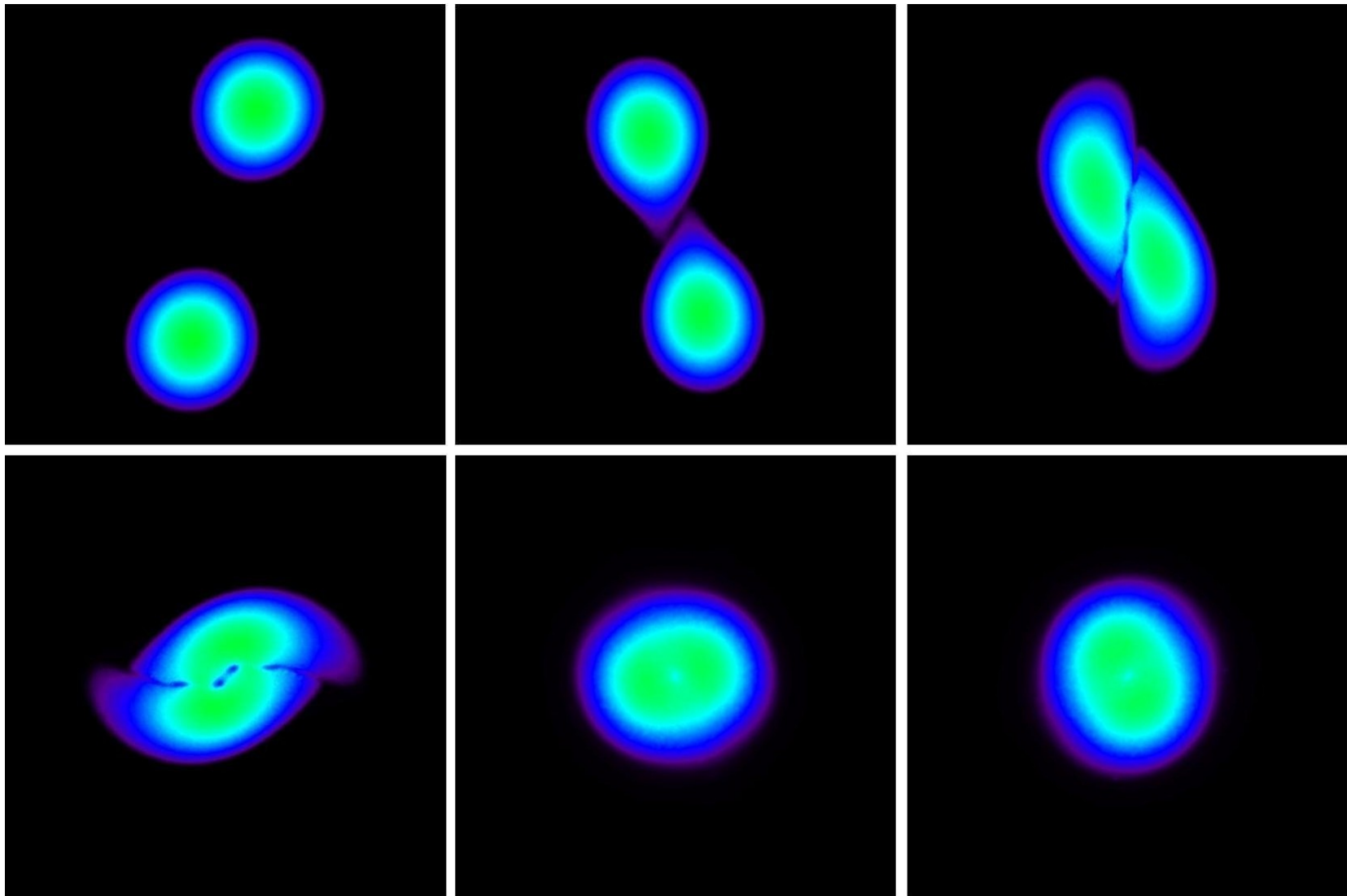


42 out of 47 models lead to the formation of a differentially rotating NS (only one accepted EoS leads to prompt collapse)



Rest-mass density, equatorial plane, 1.35-1.35 Msun, Shen EoS

Simulation: snapshots

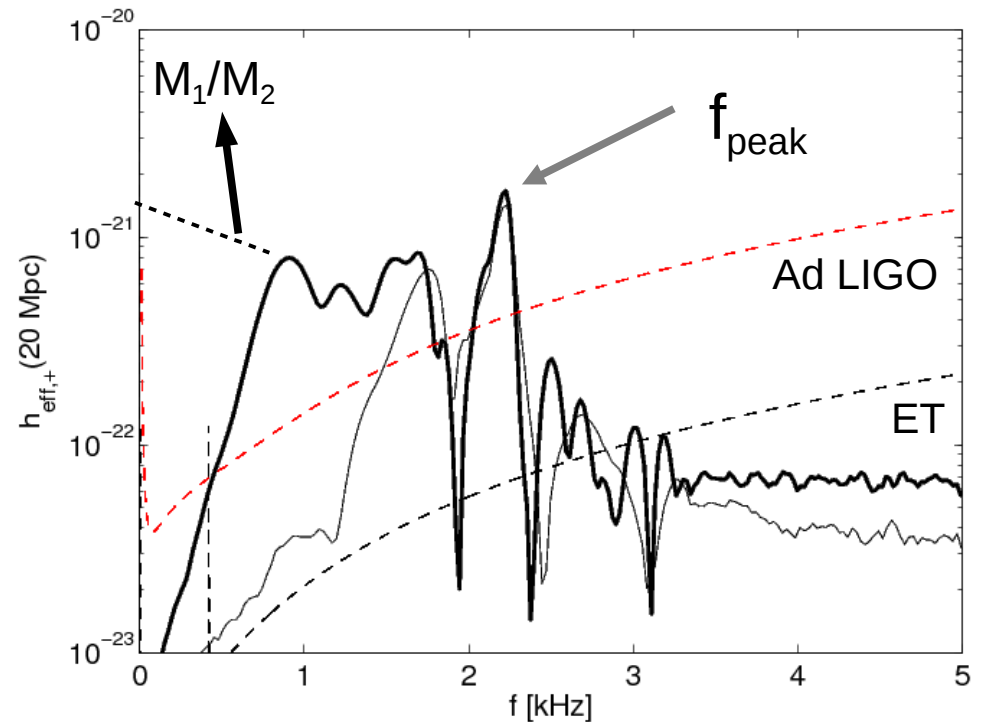
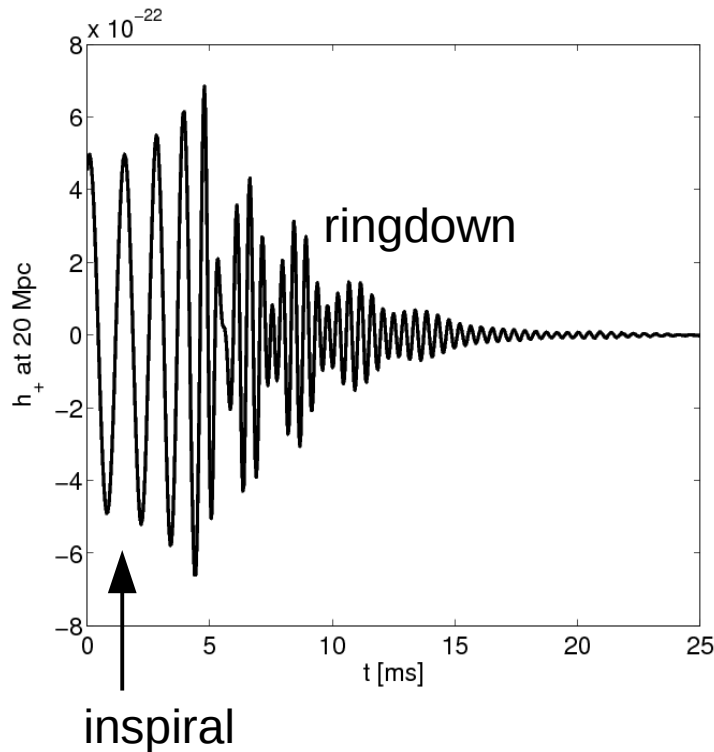


- Rest-mass density evolution in equatorial plane: $1.35-1.35 M_{\text{sun}}$ Shen EoS
- (Smooth Particle Hydrodynamics; conformal flatness condition for Einstein eqs.)

Gravitational-wave spectrum

1.35-1.35 M_{sun} Shen equation of state (EoS), 20 Mpc

$$h_{\text{eff}} = \tilde{h}_{\text{eff}}(f) \cdot f$$

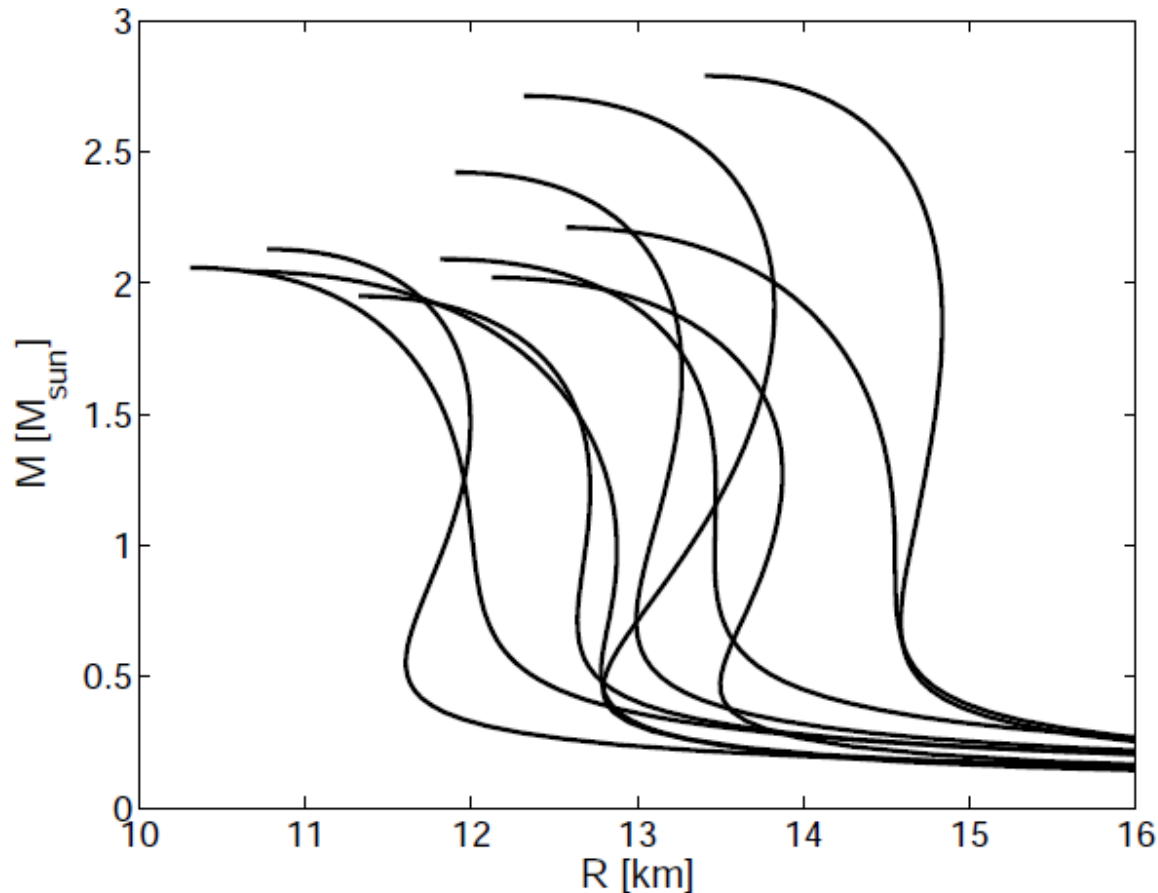


Pronounced peak in the kHz range as a **robust feature** of all models forming a differentially rotating NS

f_{peak} as the strongest feature of the postmerger phase characterizes GWs

h via quadrupole formula (also more sophisticated extraction mechanisms)

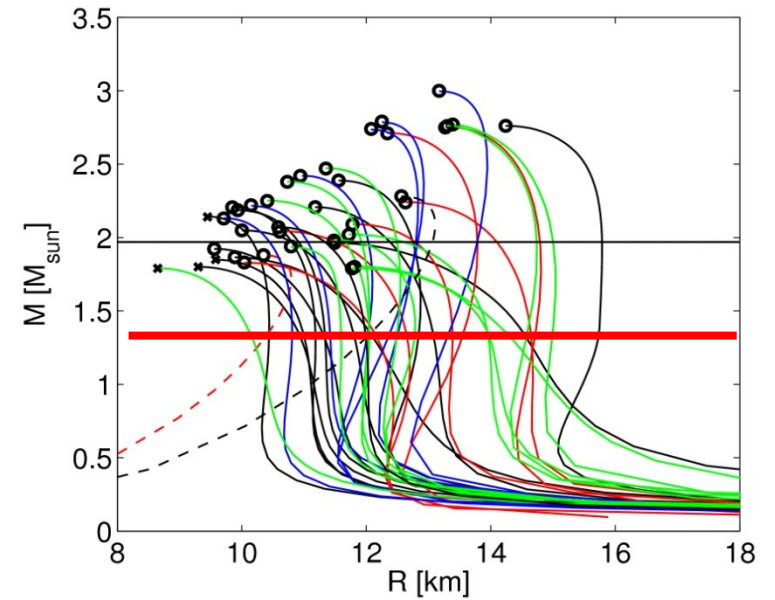
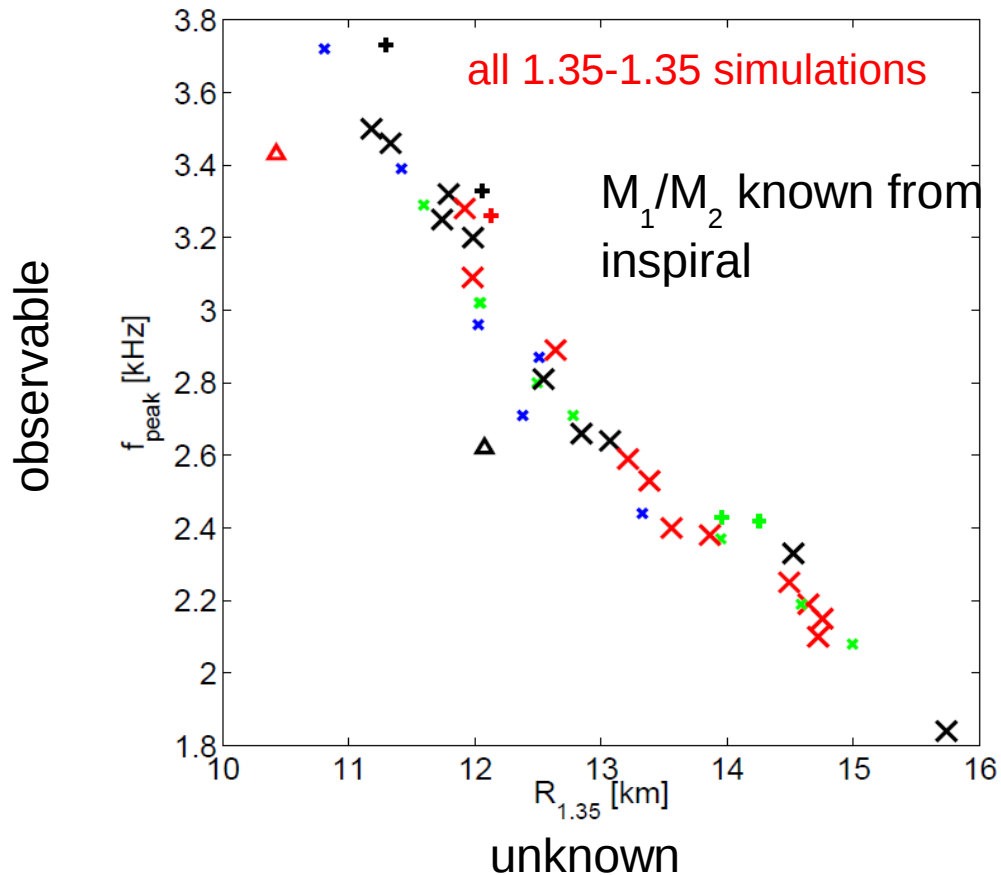
Set of simulations $\rightarrow f_{\text{peak}}$ for different EoS



EoS (Ref.)	f_{peak} [kHz]
NL3 [70, 71]	2.15
LS375 [73]	2.39
DD2 [71, 74]	2.62
TM1 [68, 69]	2.25
SFHX [75]	3.09
GS2 [76]	2.55
SFHO [75]	3.29
LS220 [73]	2.89
TMA [69, 77]	2.38
IUF [71, 78]	2.88

for 1.35-1.35 M_{sun} binary mergers
 representative sample of EoSs

Gravitational waves – EoS survey

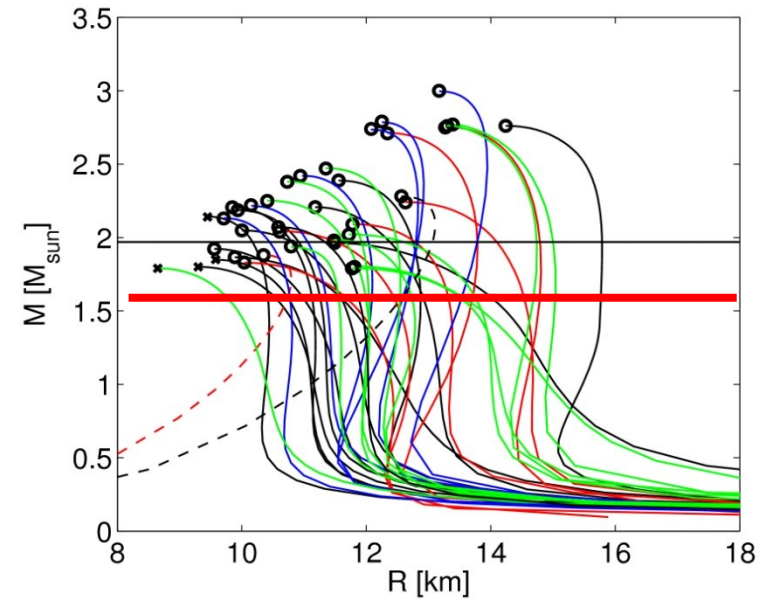
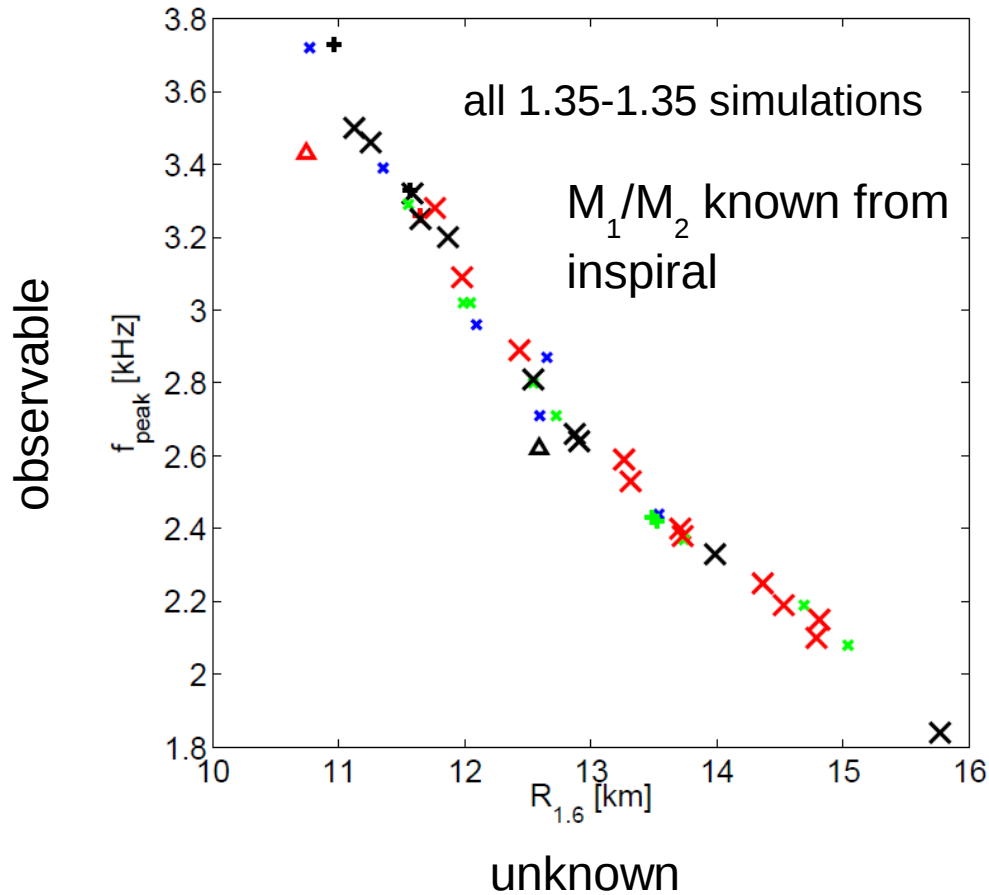


characterize EoS by radius of nonrotating NS with $1.35 M_{\text{sun}}$

Triangles: strange quark matter; red: temperature dependent EoS; others: ideal-gas for thermal effects

Bauswein et al. 2012

Gravitational waves – EoS survey



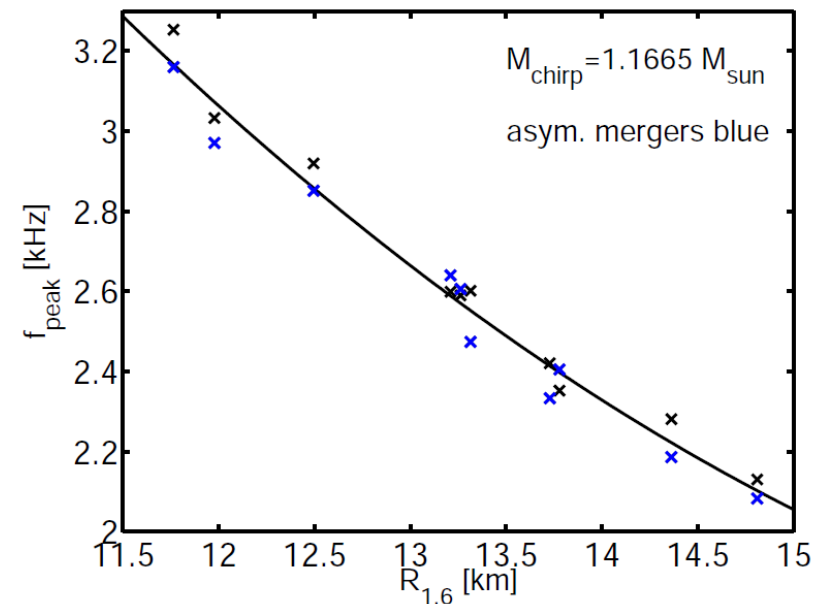
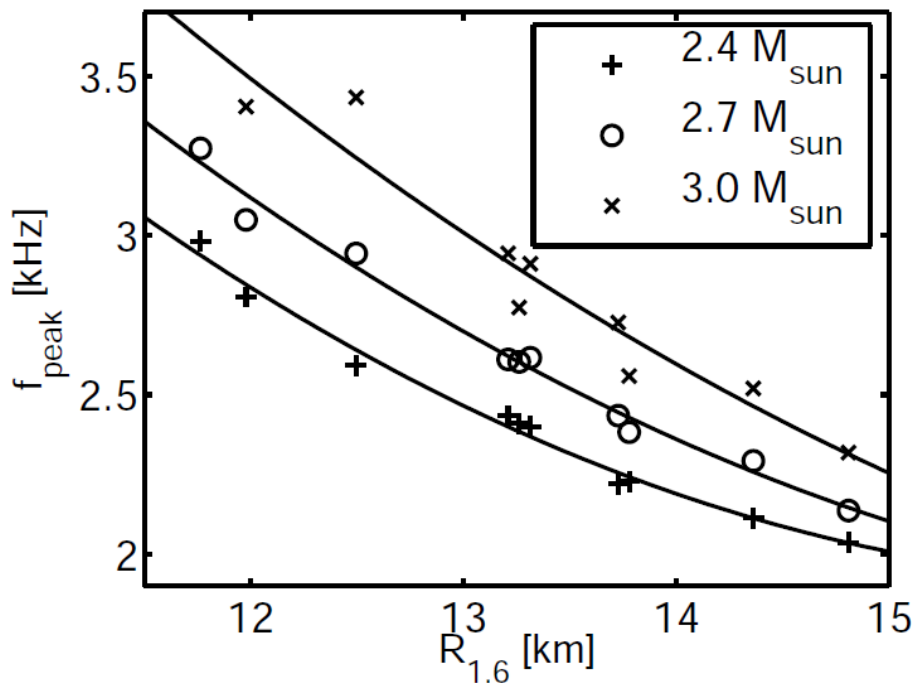
characterize EoS by radius of nonrotating NS with $1.6 M_{\text{sun}}$

Triangles: strange quark matter; red: temperature dependent EoS; others: ideal-gas for thermal effects

Bauswein et al. 2012

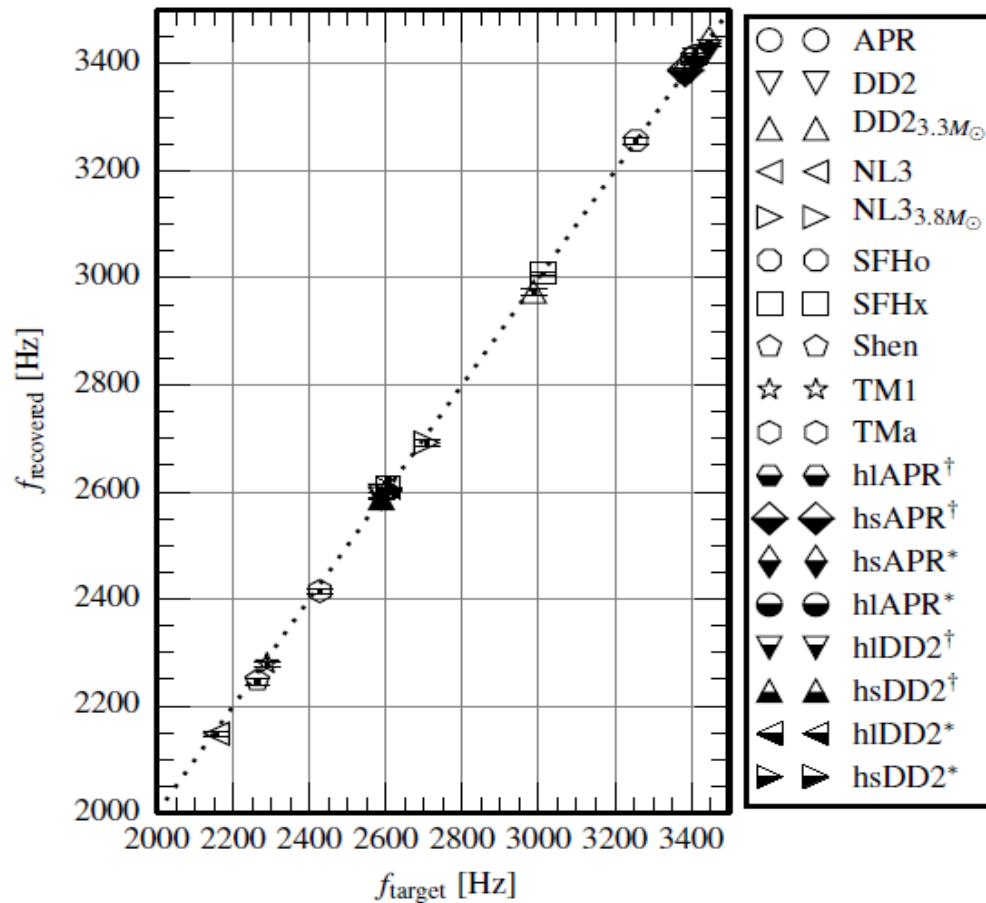
Remarks: Radius measurement via postmerger phase

- Very small scatter allows very accurate **radius detection** (= simultaneous mass and radius measurement)
- Similar relations for other binary masses and asymmetric systems
- Recall: **masses are measurable from inspiral** → choose the relation to convert f_{peak} to radius



If only M_{chirp} is used

Measuring the dominant GW frequency



Model waveforms hidden in rescaled LIGO noise

Peak frequency recovered with burst search analysis

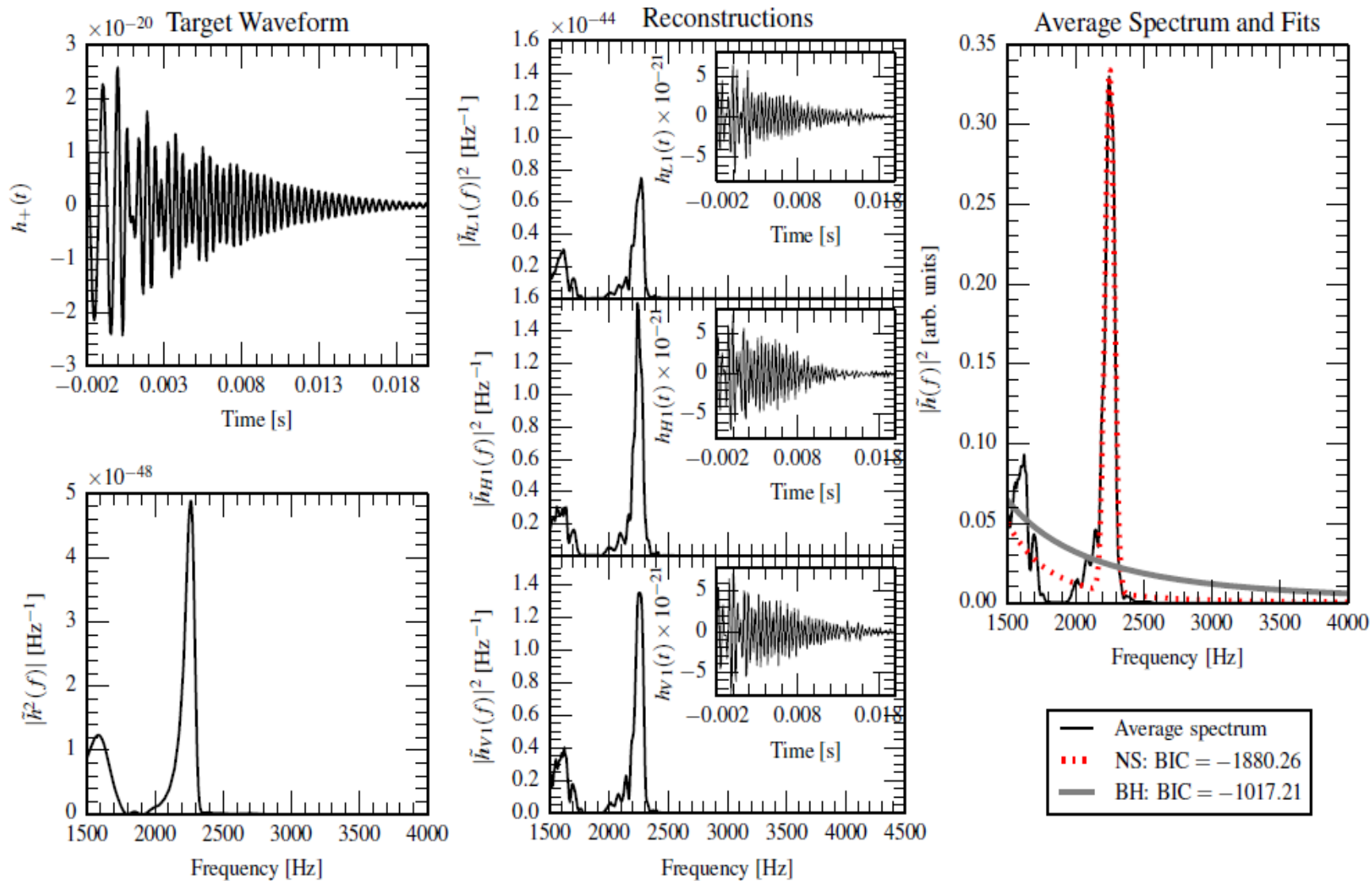
Error ~ 10 Hz

For signals within ~10-25 Mpc

=> for near-by event radius measurable with high precision (~0.01-1/yr)

- Proof-of-principle study
- → improvements likely, PCA, template based search

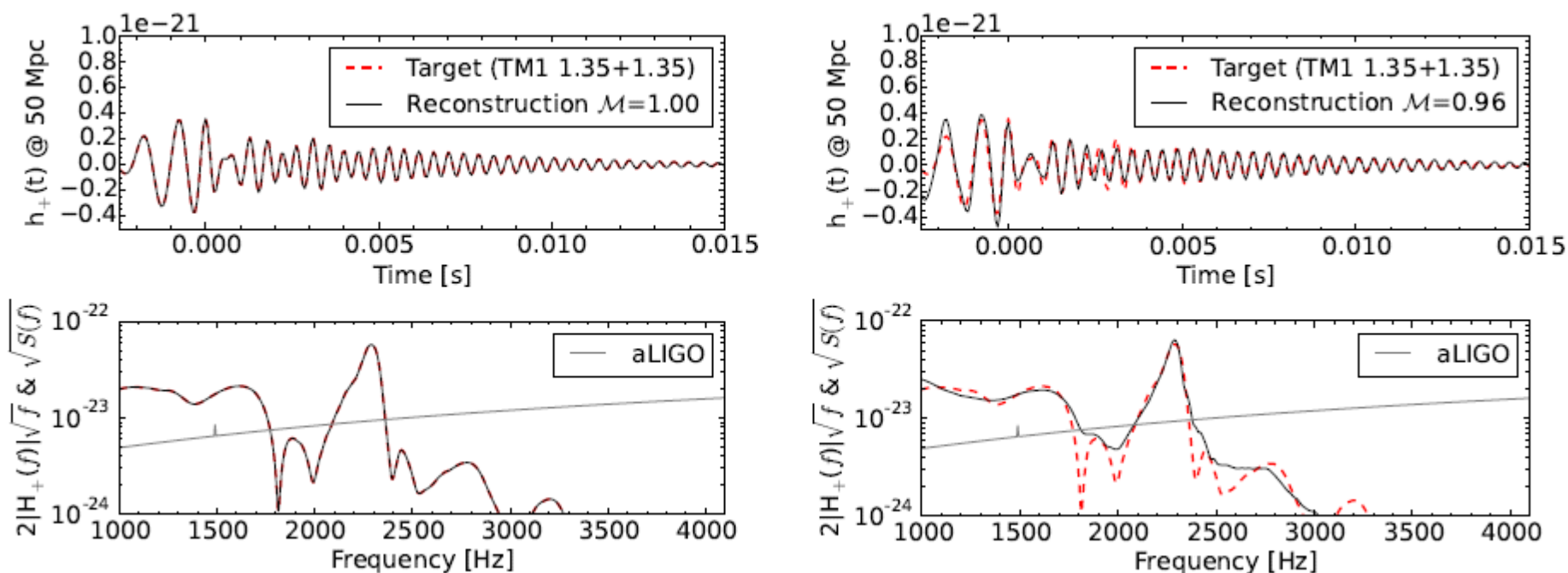
Clark et al. 2014



Discrimination between prompt collapse and delay/no collapse possible

Shen 1.35-1.35; Clark et al. 2014

Principal component analysis



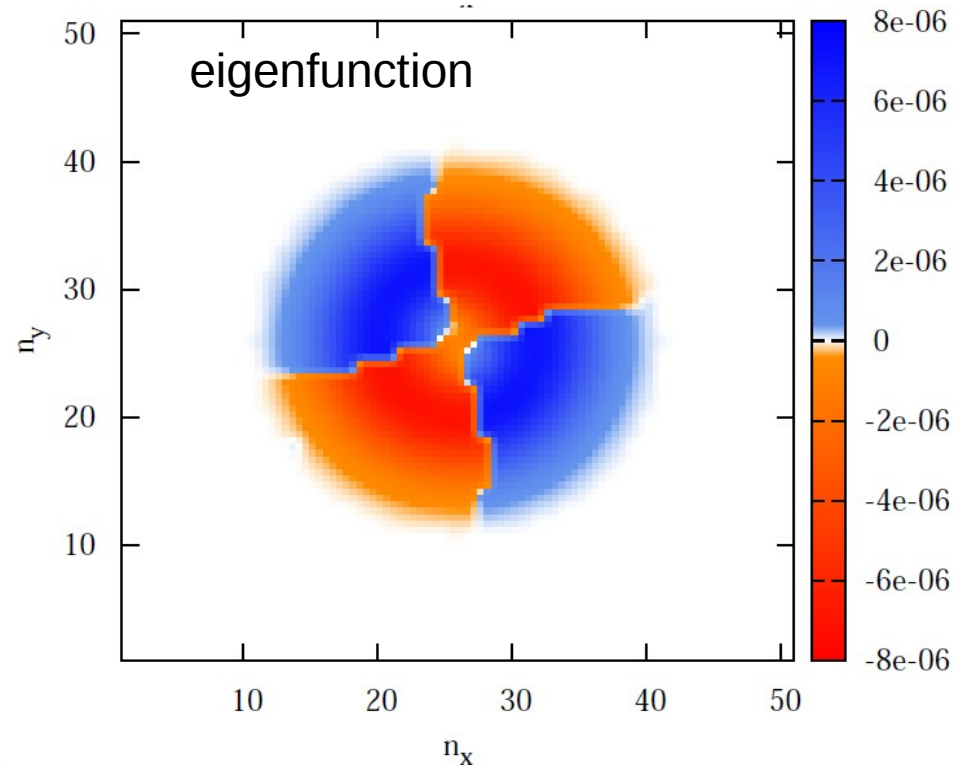
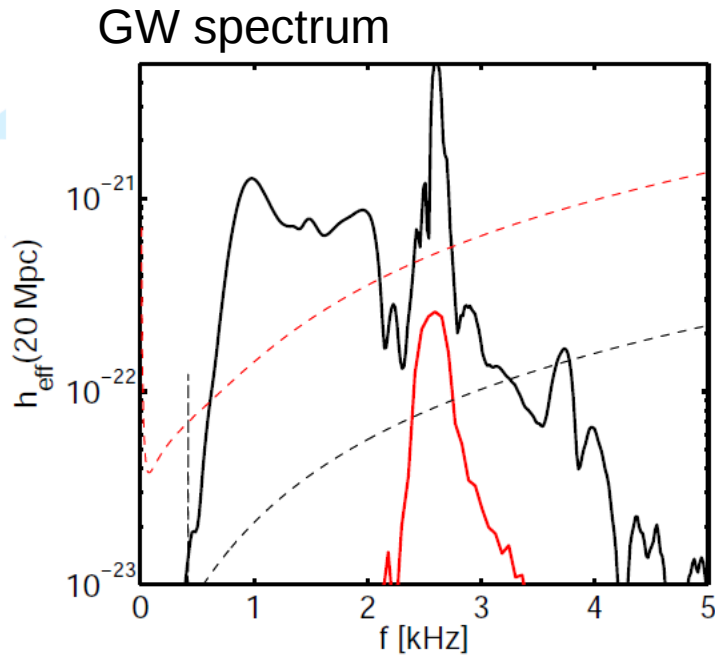
Improvement compared to morphology-independent search by many 10 % in range(!) (recall impact on rates)

Instrument	SNR_{full}	SNR_{post}	D_{hor} [Mpc]	$\dot{\mathcal{N}}_{\text{det}}$ [year^{-1}]
aLIGO	2.99 ^{3.86} _{2.37}	1.48 ^{1.86} _{1.13}	29.89 ^{38.57} _{23.76}	0.01 ^{0.03} _{0.01}
A+	7.89 ^{10.16} _{6.25}	4.19 ^{5.35} _{3.26}	78.89 ^{101.67} _{62.52}	0.13 ^{0.20} _{0.10}
LV	14.06 ^{18.13} _{11.16}	7.28 ^{9.30} _{5.64}	140.56 ^{181.29} _{111.60}	0.41 ^{0.88} _{0.21}
ET-D	26.65 ^{34.28} _{20.81}	12.16 ^{15.31} _{9.34}	266.52 ^{342.80} _{208.06}	2.81 ^{5.98} _{1.33}
CE	41.50 ^{53.52} _{32.99}	20.52 ^{25.83} _{15.72}	414.62 ^{535.22} _{329.88}	10.59 ^{22.78} _{5.33}

Adopting a “realistic” rate (uncertain)

Clark et al 2015

Nature of f_{peak}



$$\delta v_\theta = 0.4 \sin\left(\pi \frac{r}{r_{\text{surface}}(\theta)}\right) \sin(\theta) \cos(\theta) \cos(2\phi),$$

Stergioulas et al 2011

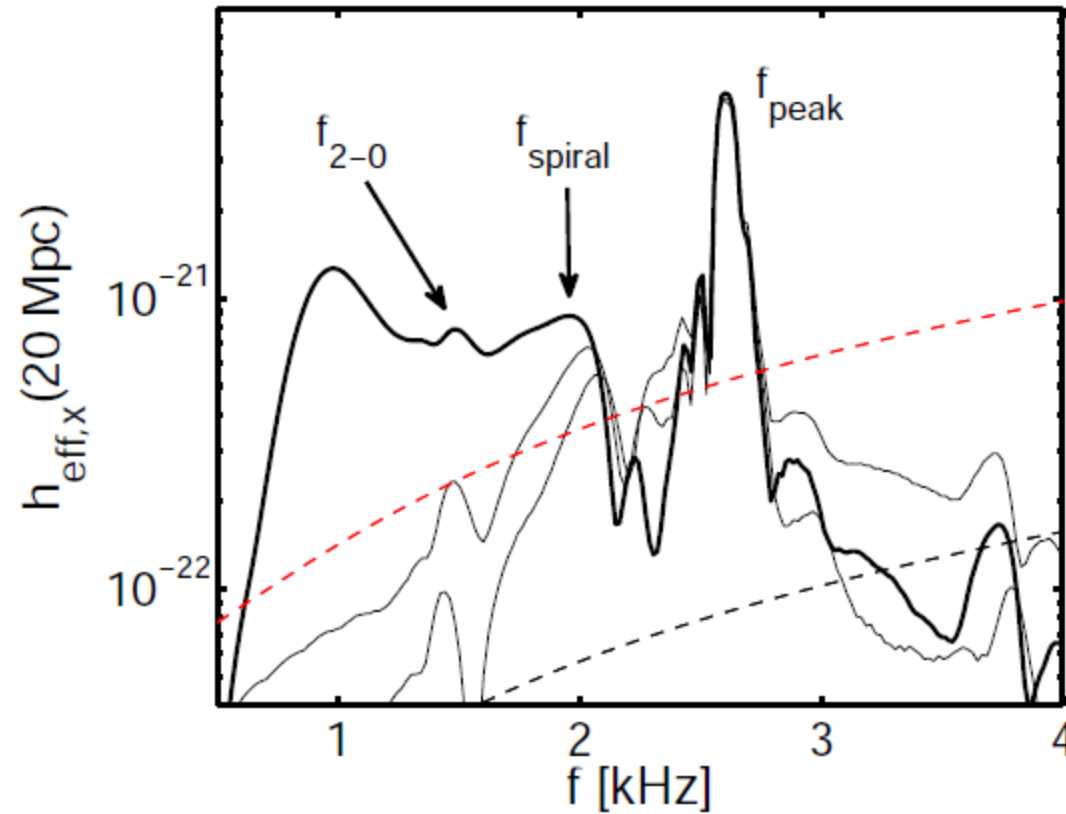
Bauswein et al. 2015

- f_{peak} is the fundamental quadrupolar fluid mode (**f-mode**)
- Reexcite f-mode

$$f_{peak} \sim \sqrt{\frac{M_{tot}}{R_{rem}^3}} \quad \Rightarrow \quad f_{peak} \sim \sqrt{\frac{M_{tot}}{R_{1.6}^3}}$$

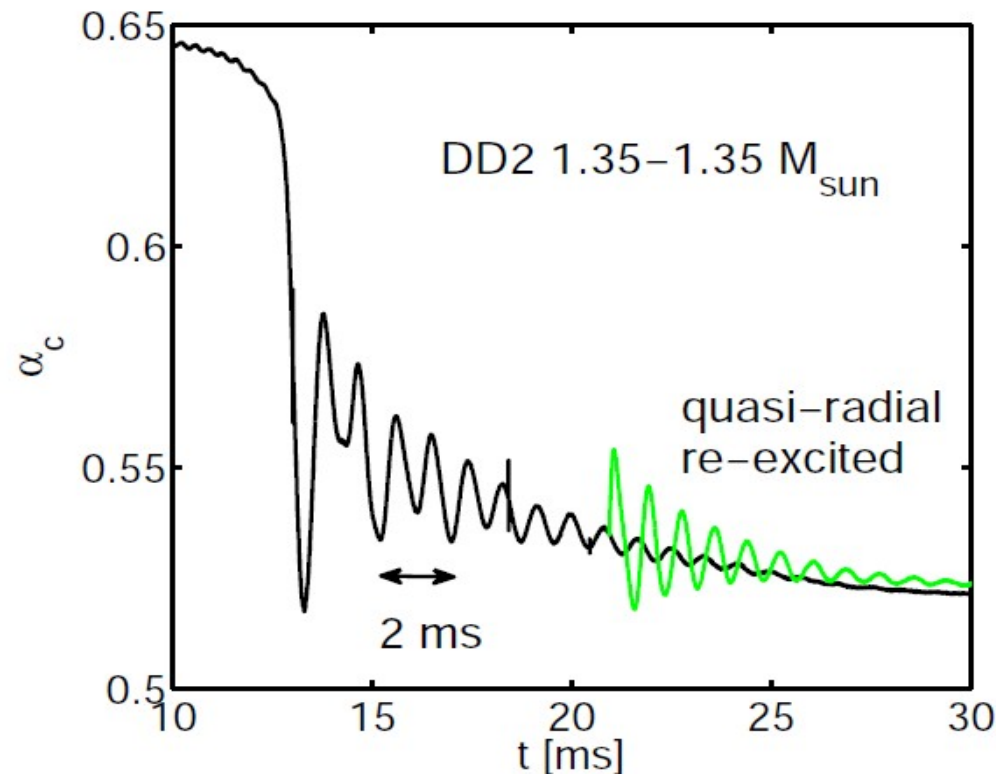
Secondary GW peaks and oscillation modes

Secondary features of the spectrum



Mode interaction: f2-0

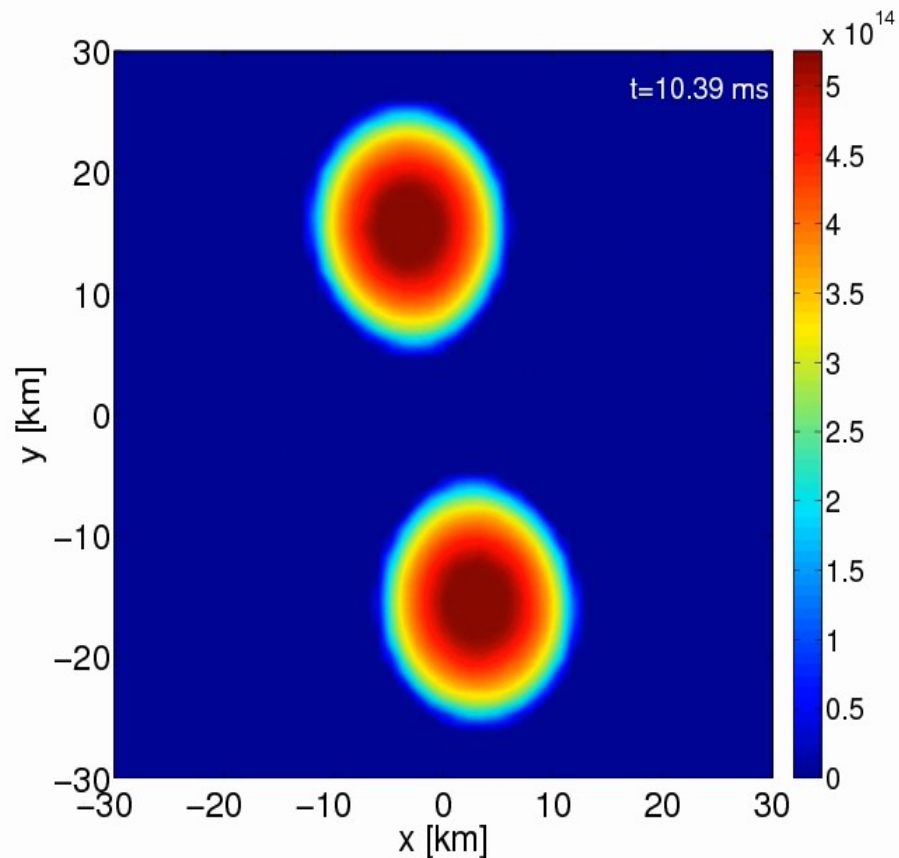
- **Radial oscillation mode:** f_0 (does not radiate GWs), but seen e.g. in central lapse function (relativistic analog of gravitational potential)
- But **couples to fpeak** (f-mode) \rightarrow peak at $f_{2-0} = f_{\text{peak}} - f_0$ (and another side peak at higher frequencies $f_{2+0} = f_{\text{peak}} + f_0$) Stergioulas et al 2011



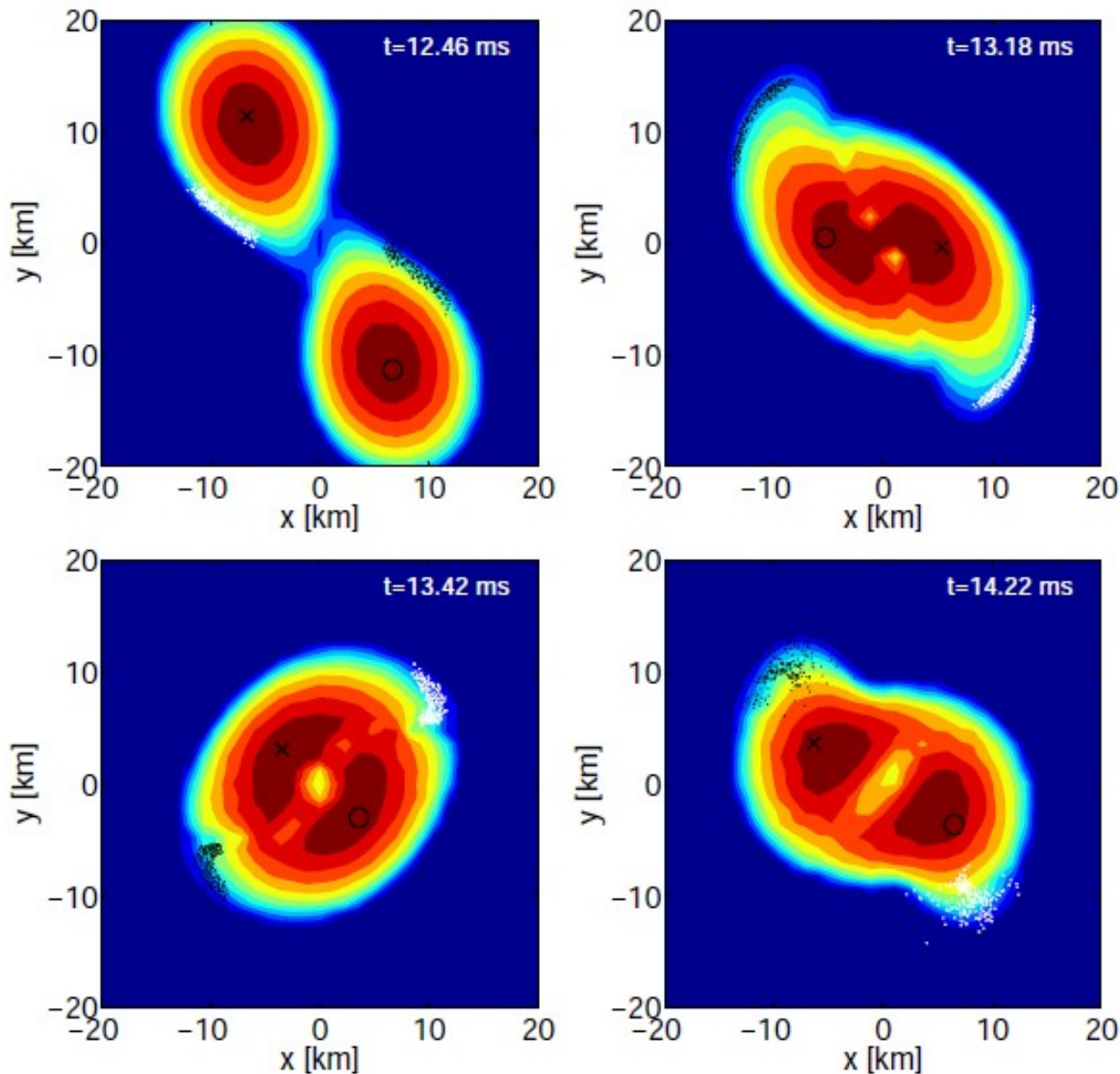
Bauswein et al 2015

Secondary GW peak fspiral

- During merging: **bulges** form at the outer edge of the remnant
- **Orbital motion** generates GWs at $f_{\text{spiral}} = 2 * f_{\text{orbit bulges}}$



Antipodal bulges (spiral pattern)



Orbital motion of antipodal bulges slower than inner part of the remnant (double-core structure)

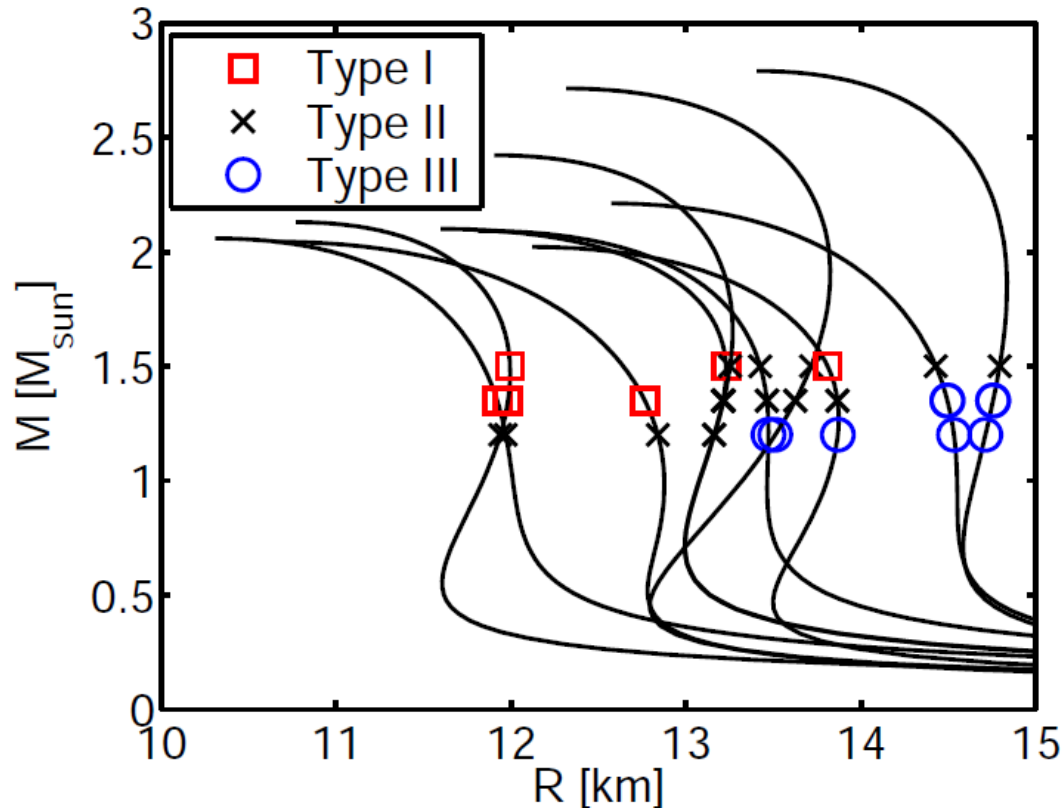
Spiral pattern, created during merging lags behind

Orbital frequency: $1/1\text{ms} \rightarrow$ generates GW at 2 kHz !!!

Present for only a few ms / cycles

Remarks:

- Presence and strength of secondary peaks depends in particular way on EoS and Mass (f_{peak} always present) → [classification system of GW spectra](#): three different types can be identified
- Also frequencies secondary peaks show EoS and mass dependence (helpful)



Summary: Overview and GWs

- **NS binaries are expected to merge** (due to GW emission); event rate uncertain but probably observational significant
- Merger phases: inspiral (chirp, increasingly faster) – merging - postmerger
- GW detectors (already operational) **measure binary masses** (in particular **chirp mass**)
- For nearby events: **GW inspiral** (last cycles) measures **tidal deformability** to discern different EoSs
- For nearby events: **postmerger** remnant shows **characteristic peaks** in GW spectrum
- Main peak by remnant's f-mode scales with radii of non-rotating NS → accurate **radius measurements** possible
- Main peak detectable
- Certain mechanisms generate **secondary peaks**, e.g. oscillation mode interaction, antipodal deformations

Not covered:

- **Collapse behavior** → determination of maximum mass of non-rotating NSs

Collapse behavior:

Prompt vs. delayed (/no) collapse

Relevant for:

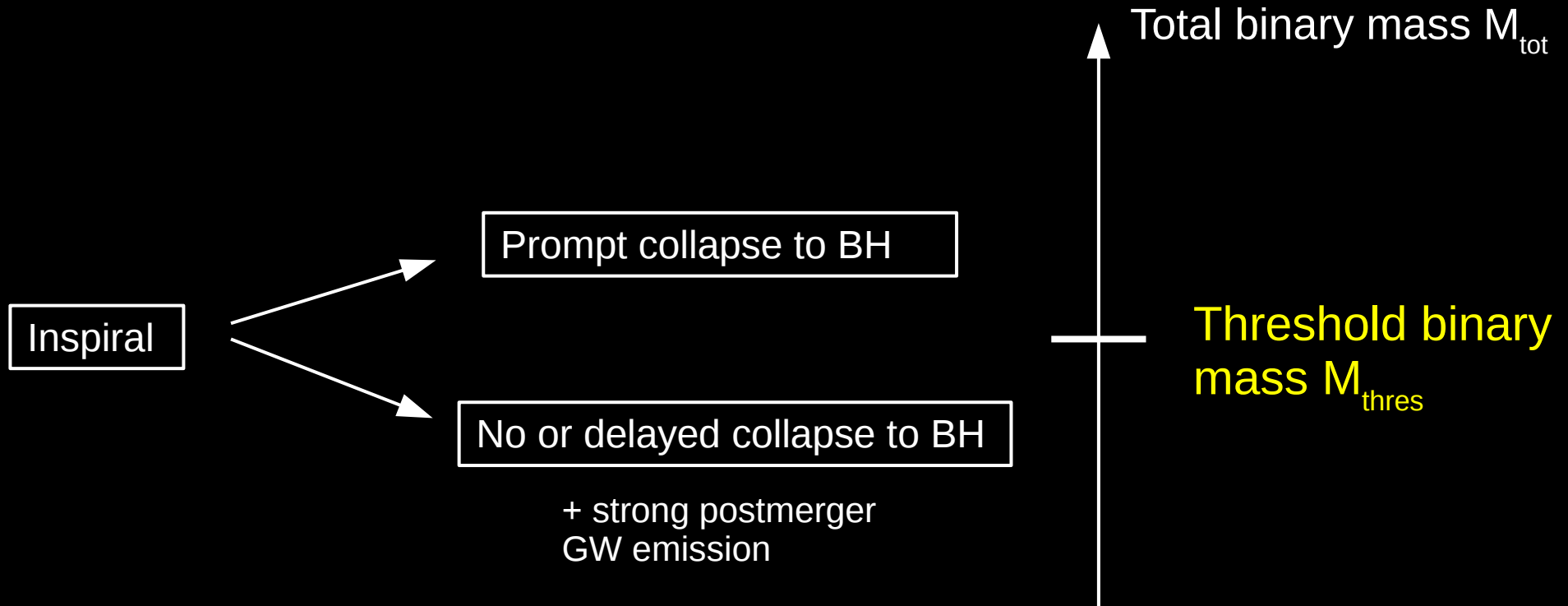
EoS constraints through M_{max} measurement

Conditions for short GRBs

Mass ejection

Electromagnetic counterparts powered by thermal emission

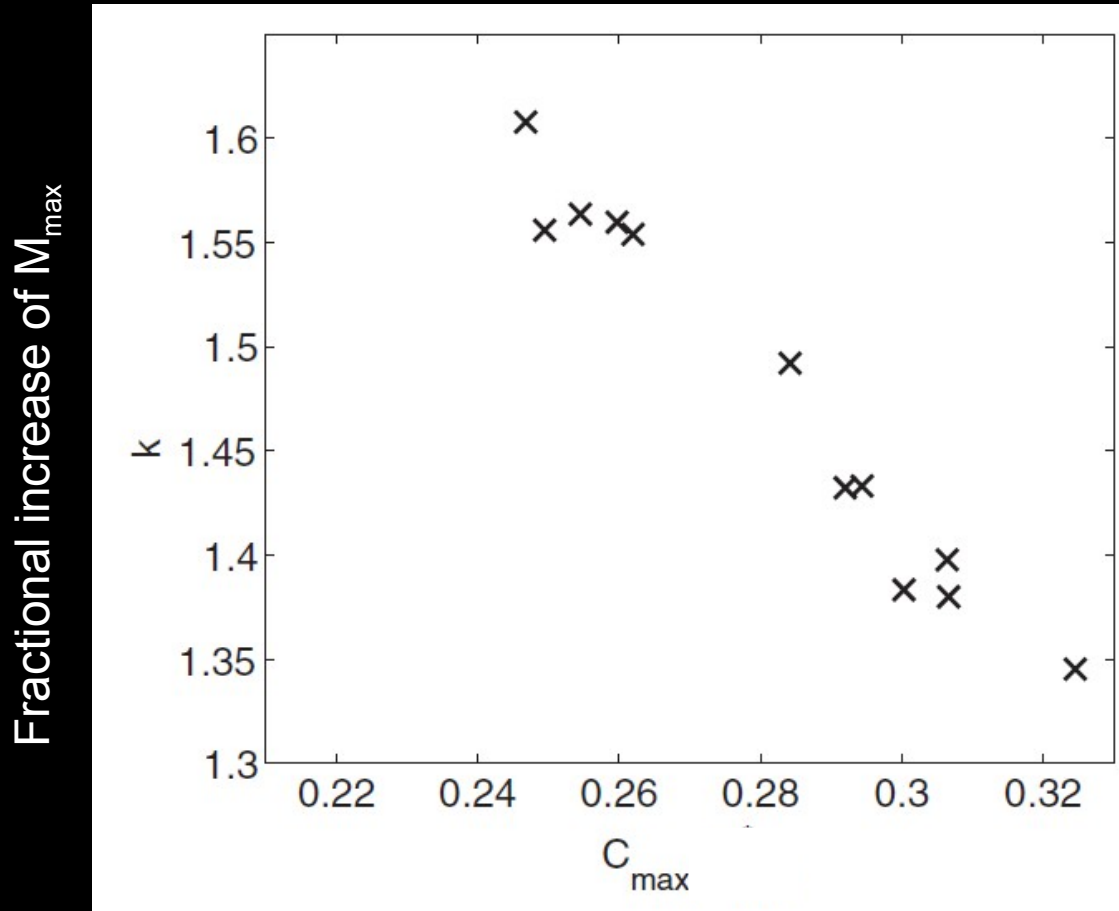
Collapse behavior



EoS dependent - somehow M_{max} should play a role

→ ... from observations we can determine M_{max} , R_{max} , ρ_{max}

Key quantity: **Threshold binary mass M_{thres}** for prompt BH collapse



$$M_{\text{thres}} = k * M_{\text{max}}$$

with $k = k(C_{\text{max}})$

$$C_{\text{max}} = G M_{\text{max}} / (c^2 R_{\text{max}})$$

(compactness of TOV maximum-mass configuration)

$$\Rightarrow M_{\text{thres}} = M_{\text{thres}}(M_{\text{max}}, R_{\text{max}})$$

Bauswein et al. 2013

$$k = \frac{M_{\text{thres}}}{M_{\text{max}}}$$

← From simulations with different M_{tot}

← TOV property of employed EoS

Constrain M_{\max}

- ▶ Measure several NS mergers with different M_{tot} – check if postmerger GW emission present

→ M_{thres} estimate

- ▶ Radius e.g. from postmerger frequency

$$M_{\text{thres}} = \left(-3.38 \frac{G M_{\max}}{c^2 R_{\max}} + 2.43 \right) M_{\max}$$

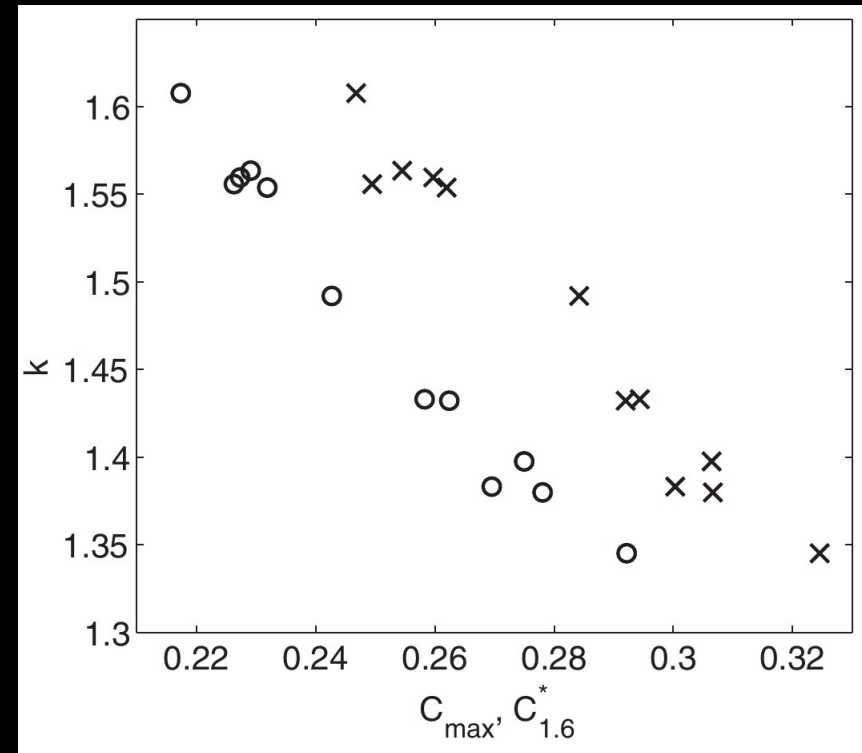
- ▶ Invert fit

$$M_{\text{thres}} = \left(-3.6 \frac{G M_{\max}}{c^2 R_{1.6}} + 2.38 \right) M_{\max}$$

→ M_{\max}

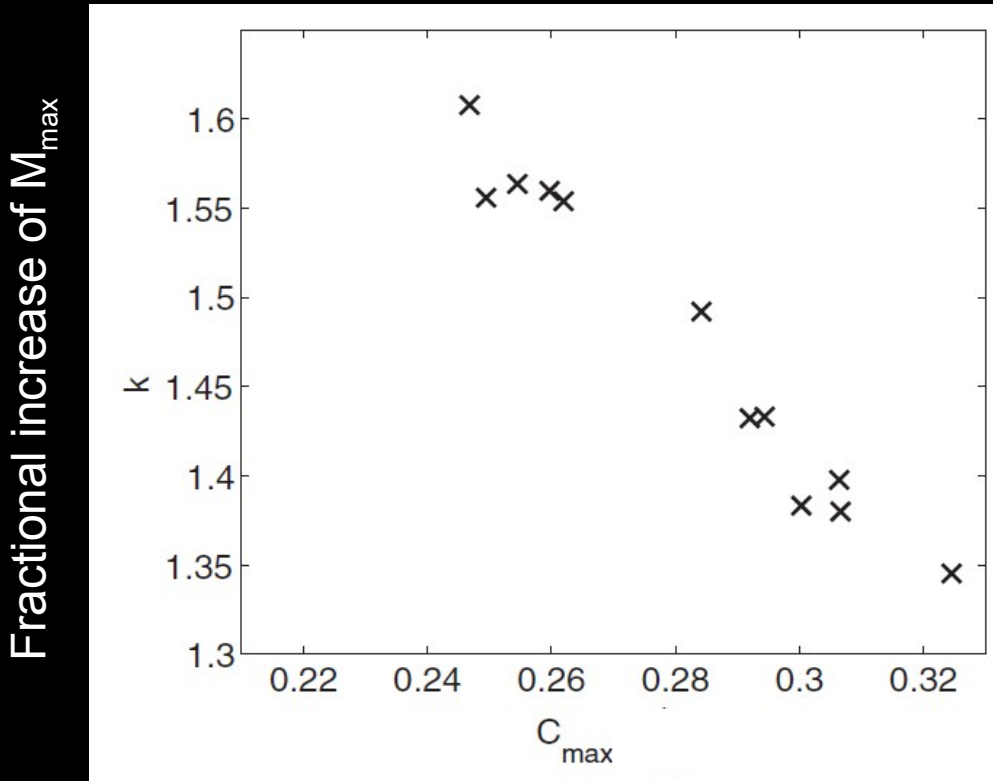
- ▶ Note: already a single/few measurement could provide interesting constraints !!!

- ▶ M_{thres} constraints also from GRB, em counterparts, ...

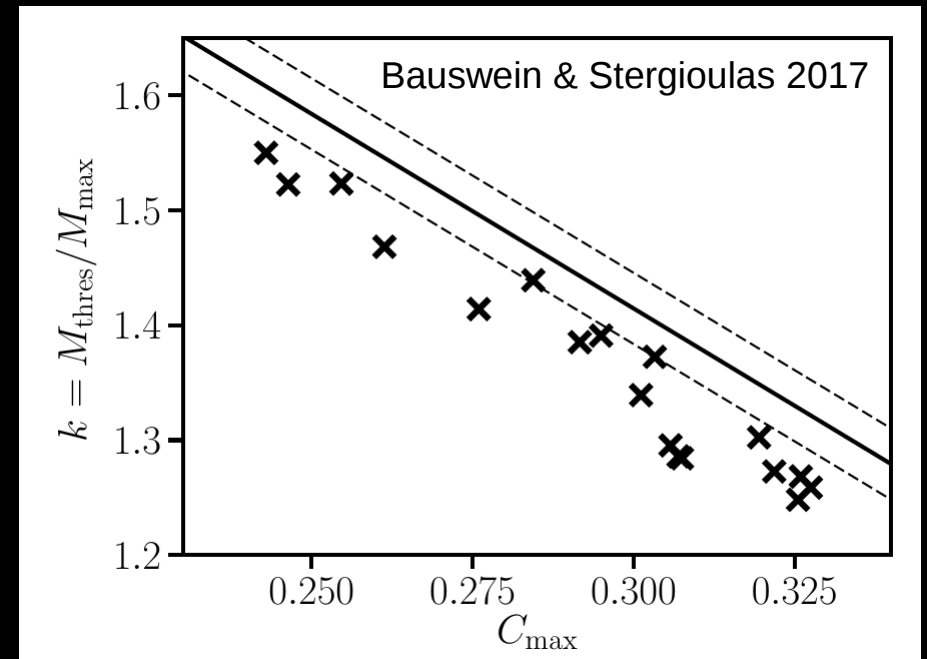


Semi-analytic model

reproduces / corroborates
collapse behavior



Bauswein et al 2013: numerical
determination of collapse
threshold through hydrodynamical
simulations



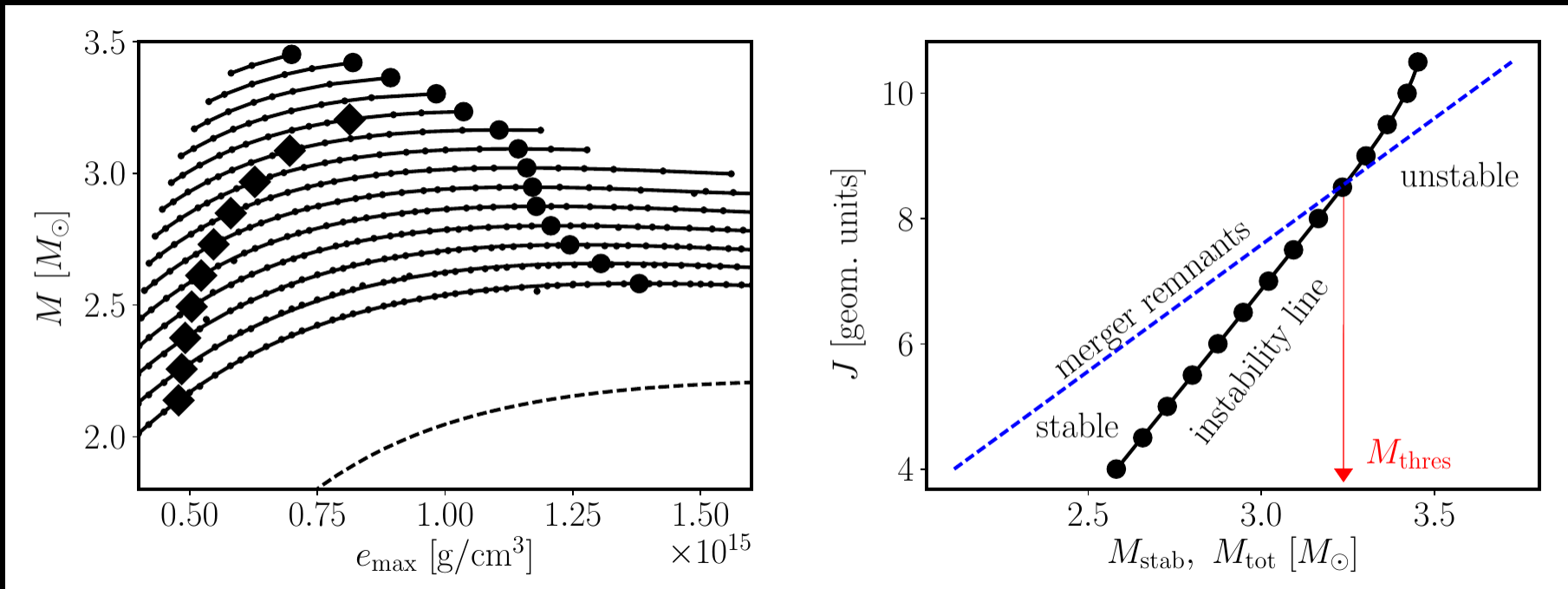
Solid line fit to numerical data

Crosses stellar **equilibrium models**:

- prescribed (simplistic) diff. rotation
- many EoSs at $T=0$
- detailed angular momentum budget !
=> equilibrium models qualitatively
reproduce collapse behavior
- even quantitatively good considering the
adopted approximations

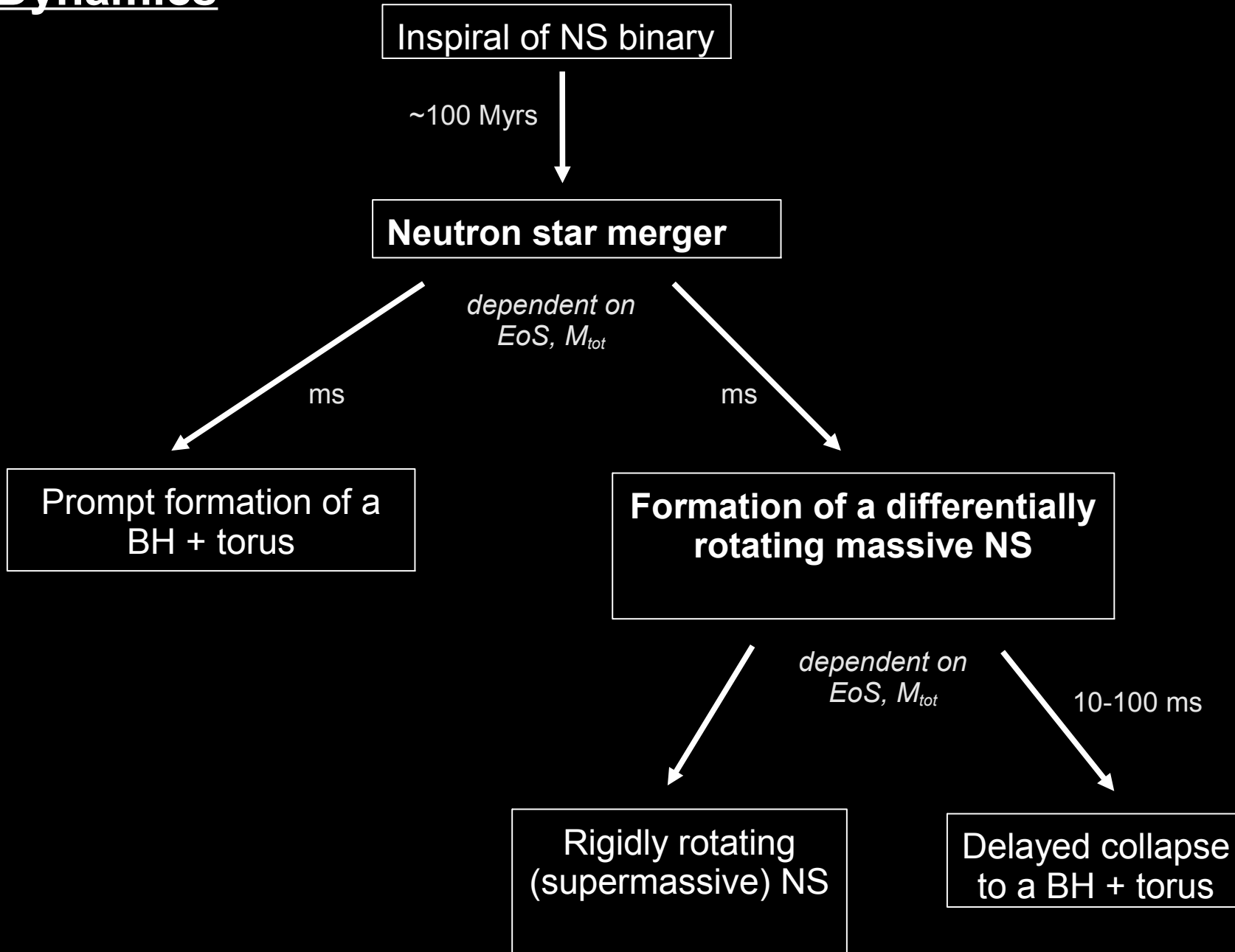
details of the model

- ▶ Stellar equilibrium models computed with RNS code (diff. Rotation, $T=0$, many different microphysical EoS) => turning points => $M_{\text{stab}}(J)$
- ▶ Compared to $J(M_{\text{tot}})$ of merger remnants from simulations (very robust result) → practically independent from simulations

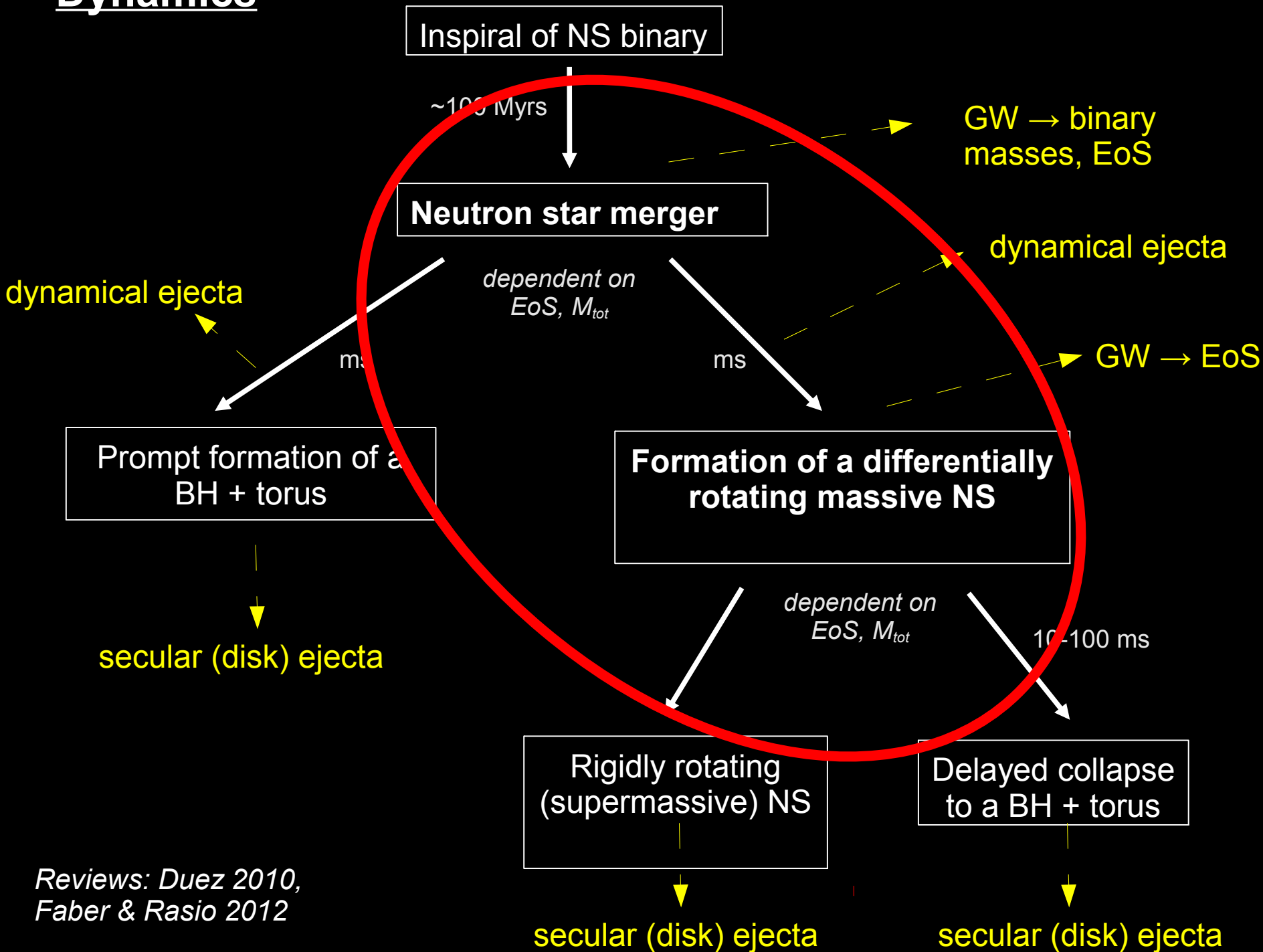


Rapid neutron-capture process

Dynamics



Dynamics



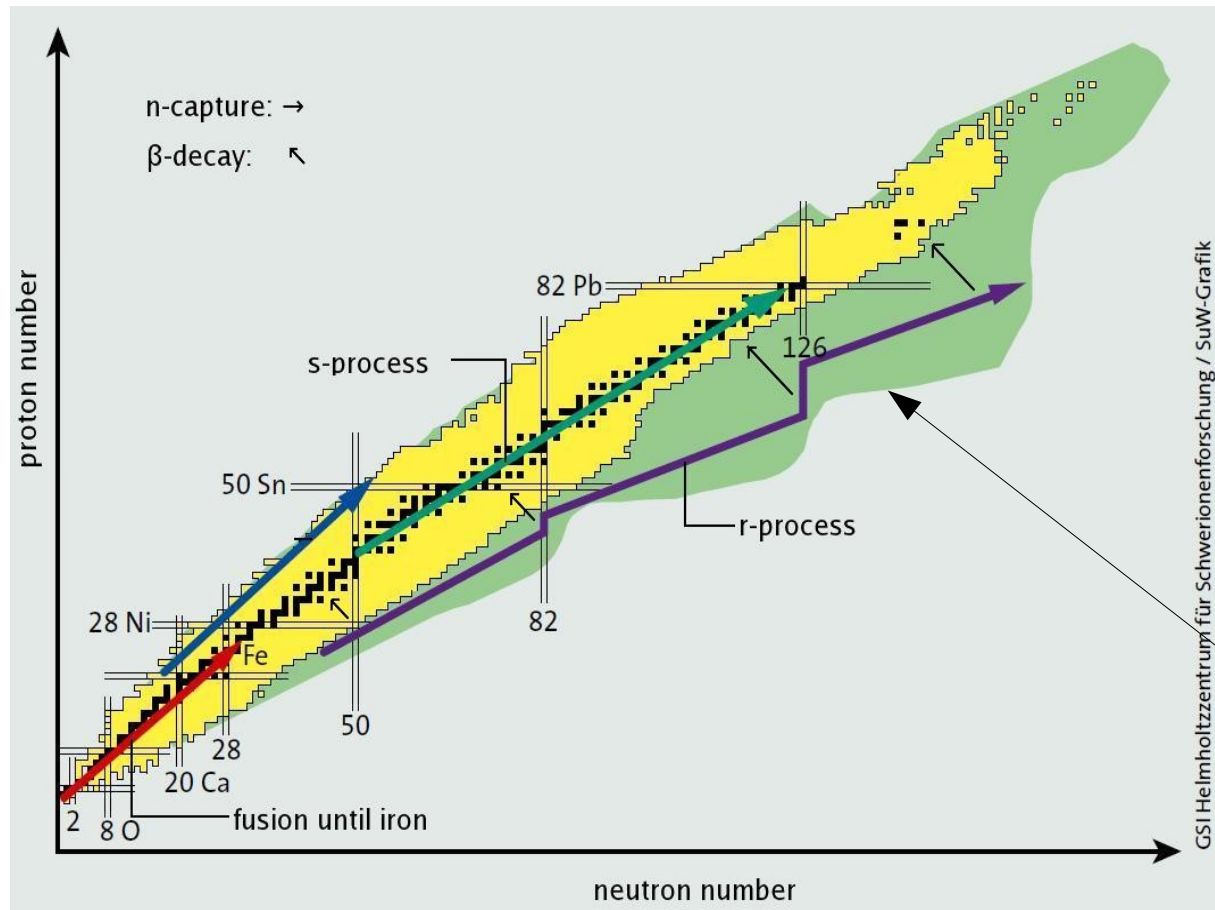
Reviews: Duez 2010,
Faber & Rasio 2012

Motivation: rapid neutron-capture process

- Explain **formation of heavy elements** – about half of all heavy nuclei
- Explain observed abundance pattern
 - solar system
 - meteorites
 - stellar atmospheres (extrasolar)
 - in particular in metal-poor stars (i.e. old stars)
- Beyond: explain cosmic, Galactic **chemical evolution**
- More subtle: understand nuclei and nuclear reactions (experimental data and **nuclear theory** → theoretically predicted abundances should match observations)
- What are the **astrophysical production sites** of the different elements? In particular, so-called r-process elements?

Neutron capture processes

High Coulomb barrier → capture neutral particle to increase atomic mass



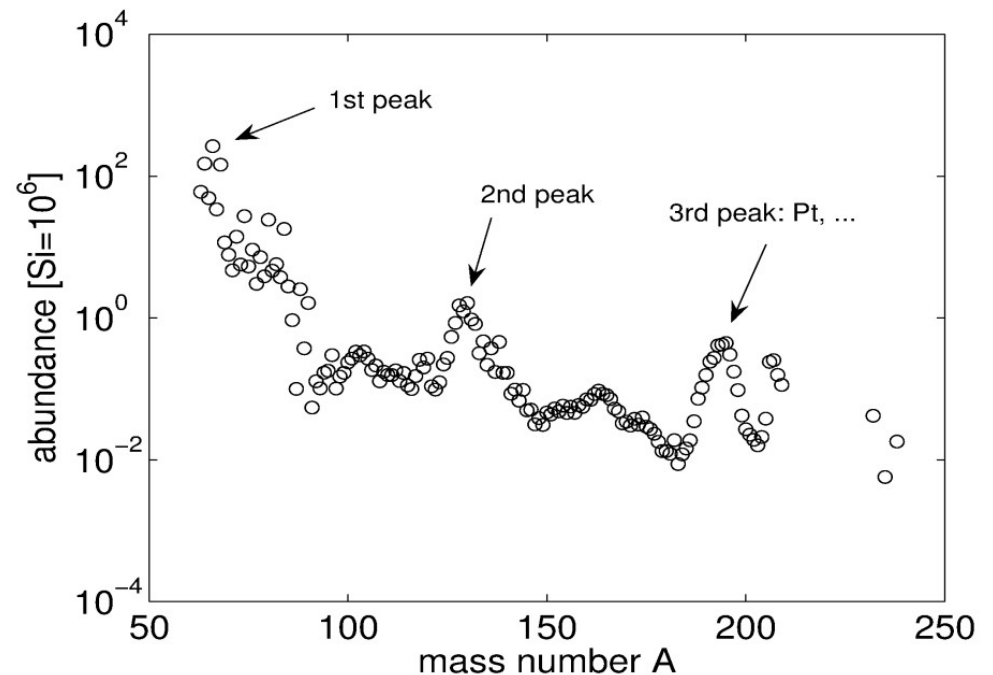
Neutron drip line
– no nuclei

To explain formation of most of the heavy elements
Site of the r-process not known

Rapid neutron-capture process

- Neutron capture processes naturally explain abundance peaks (closed neutron shells → bottle necks)
- High neutron densities required
- Particular conditions needed
 - site(s) not precisely known
- Depending on precise conditions exact details of r-process differ
- Fission may be important

Observed (s-process subtracted, some isotopes produced by both processes):



Key parameters for successful r-process

Determine the details / success of the r-process (not only in NS mergers) – parameters set by the [astrophysical environment](#)

- Electron fraction (Y_e) (= proton fraction) – measure for the neutron-richness
- Entropy - determines neutron/seed ratio
- Fast expansion time scale (to maintain neutron richness)

on top: [nuclear physics](#)

- Partially not very well known since very exotic nuclei involved – nuclear physics far away from valley of stability (not accessible by experiments – we rely on theoretical models for the reaction rates, ...)
- R-process overall relatively insensitive to nuclear physics

Discussed sites of the r-process

- Neutron-star mergers (and their remnants)
- Neutron star-black hole mergers (and their remnants)
- Dynamical ejecta of prompt exploding O-Ne-Mg core-collapse supernovae
- Neutrino-driven winds from proto-neutron stars (core-collapse supernovae)
- He- shell exposed to intense neutrino flux (during core collapse)
- Quark-novae
- Magneto-hydrodynamic jets of rare core-collapse supernovae
- ...

All have ideas/models some advantages and some disadvantages !

But overall fair to say: that mergers are very hot candidates !

(in particular since recent models of the other hot candidate (core-collapse supernovae) have difficulties to find appropriate conditions (Fischer et al. 2010, Huedepohl et al. 2010, ...))

Note: **possibly different sites** (operating simultaneously or at different times (metallicities)), different mass ranges may be produced by different sites

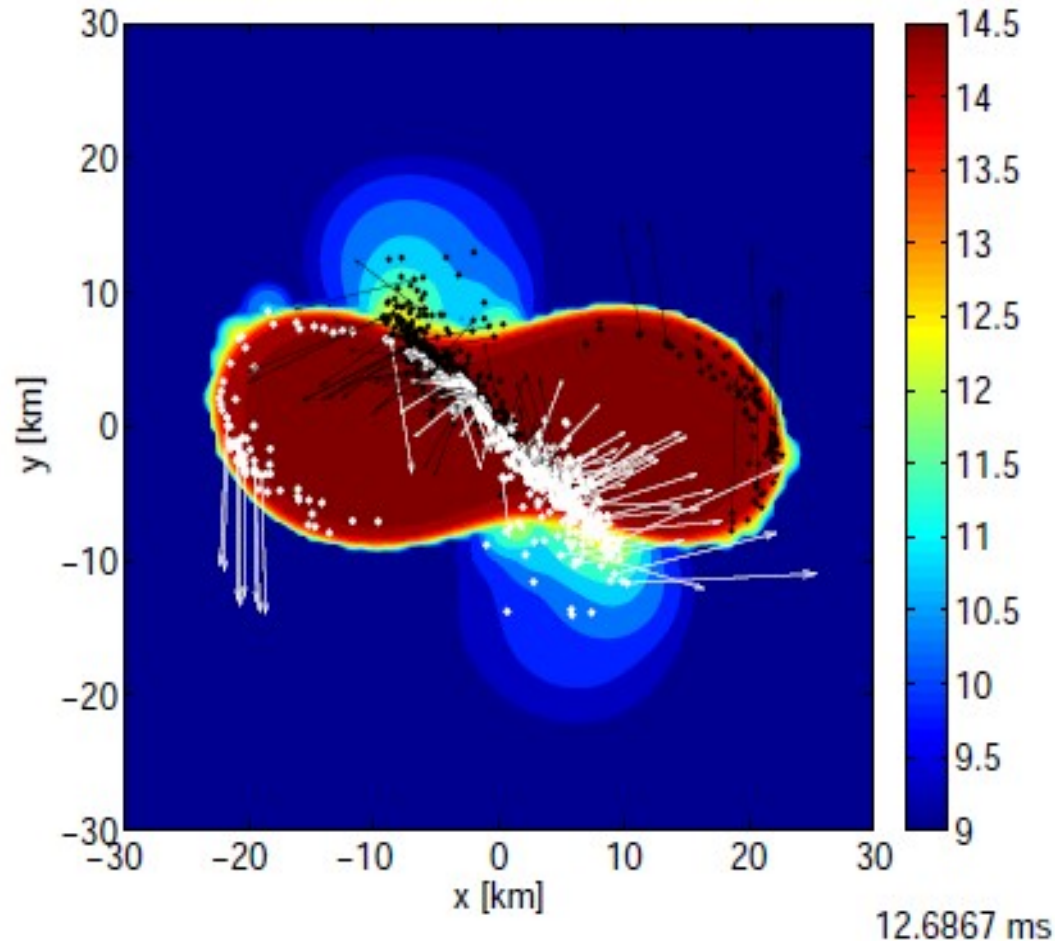
Neutron star mergers and the r-process

- Obviously: **only gravitationally unbound material of interest**
- Only accessible by numerical simulations (→ current modeling approaches)
- Important: we need to consider different types of ejecta → dynamical and secular ejecta (both can/will contribute) → overview

Different ejecta components associated with different stages

- **Dynamical ejecta** – unbound within the first milliseconds (sometimes called “prompt ejecta”)
- **Secular ejecta** – unbound on longer timescales – different effects (requires partially different modeling, e.g. only 2d for long-term simulation, more sophisticated neutrino transport, MHD, ...; sometimes called “disk ejecta/outflow”)
 - neutrino-driven ejecta (neutrinos emitted mostly from the hot central object or torus unbind matter further out)
 - viscously driven ejecta, angular momentum transport, MHD effects
- Secular ejecta is expected from both: NS merger remnant (+ torus) and BH + torus system
- Here: mostly focus on the dynamical ejecta
- Note: **very similar picture for NS-BH mergers**: dynamical + secular ejecta

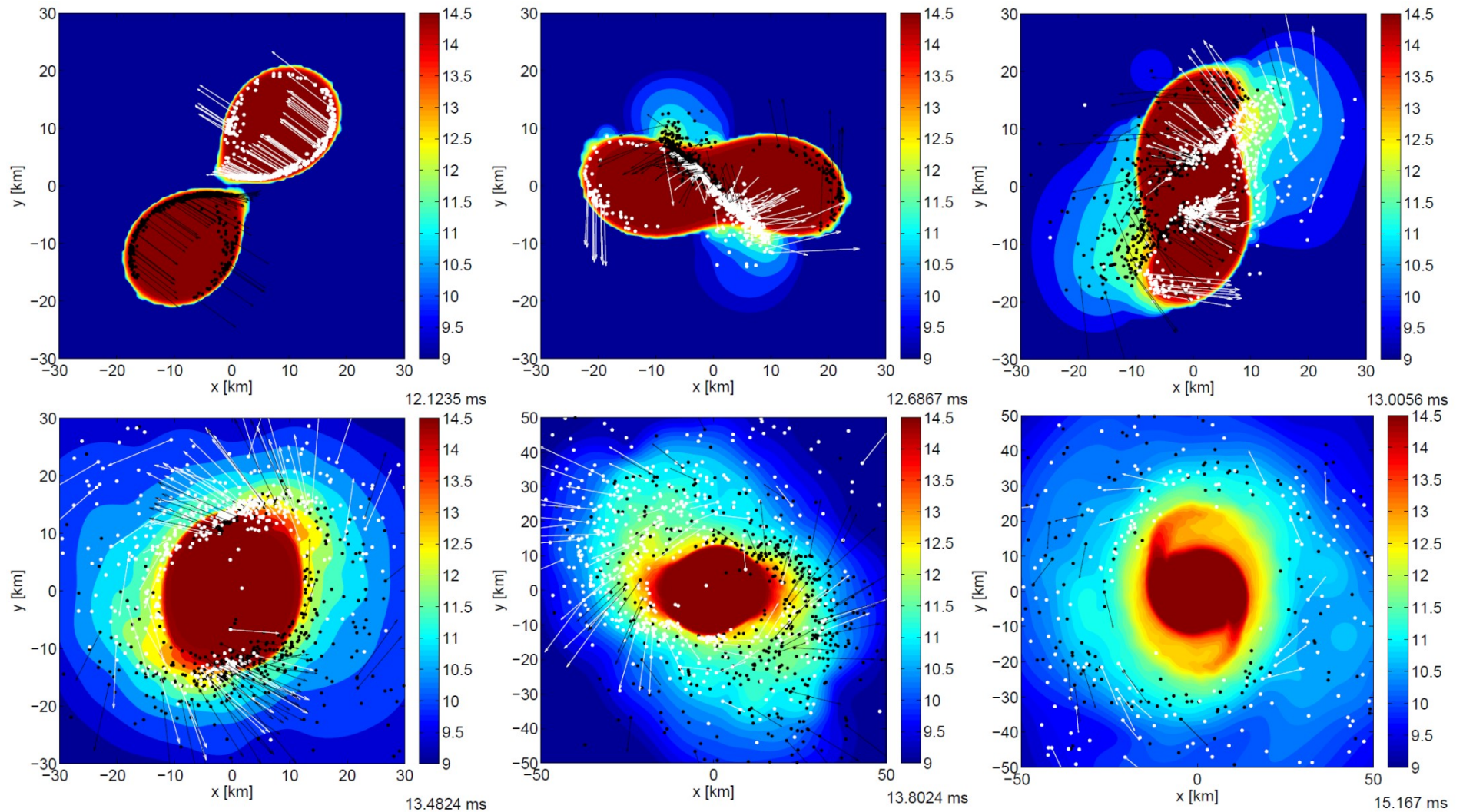
Dynamical ejecta – different types (ejection mechanisms)



Bauswein et al. 2013

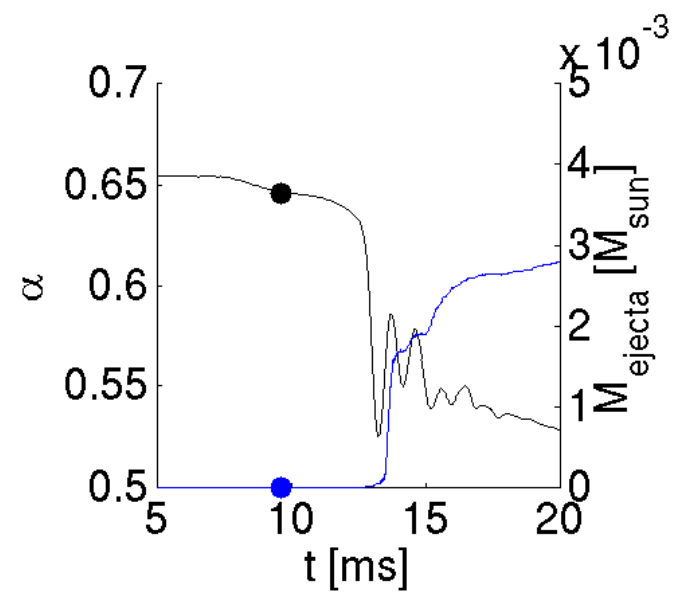
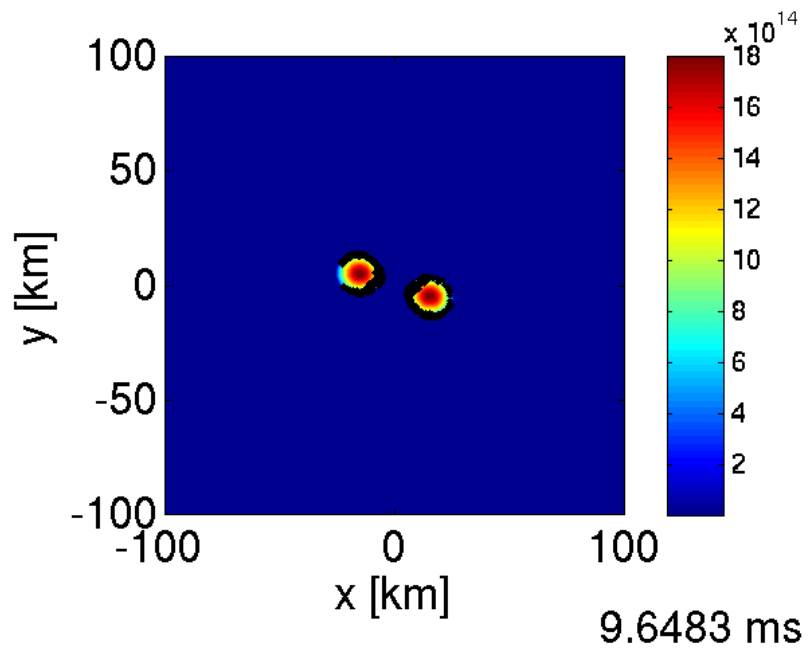
- Contact interface ejecta: shock-heated (hot, entropy)
- Tidal-tail ejecta (cold, low entropy; in particular for asymmetric systems and NSBH)
- (typical numbers for dynamical ejecta mass: $10^{-3} \dots 10^{-2} M_{\text{sun}}$)
- (torus mass $\sim 0.1 M_{\text{sun}}$ or less, \rightarrow several per cent secular ejecta)

Simulations



Every tenth unbound
fluid element

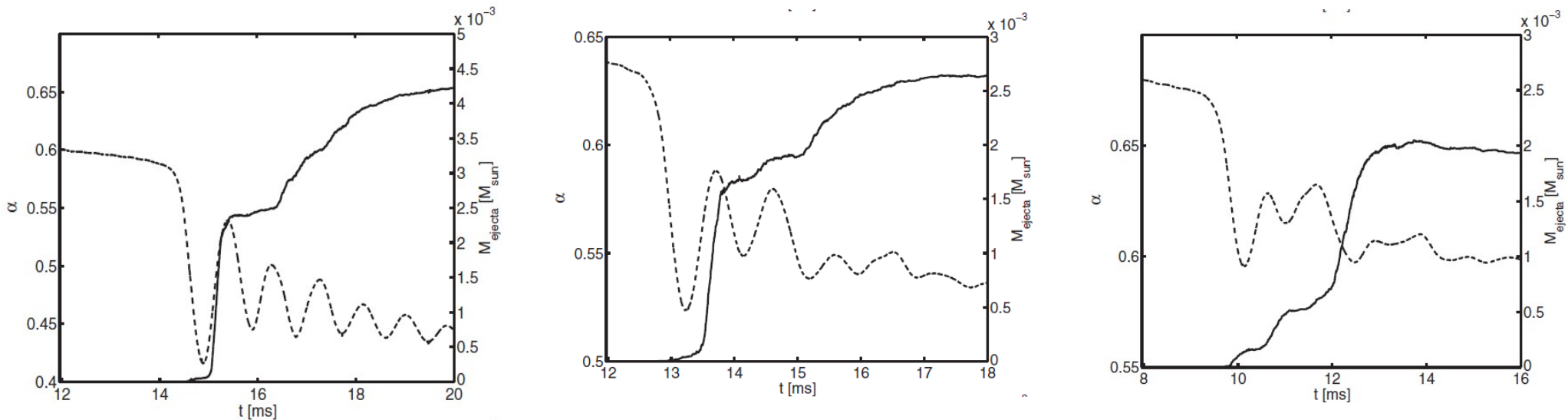
Bauswein et al. 2013



Black: bound; white: unbound (formally)
 Central lapse: measure for compactness

Ejection dynamics

- Central lapse function (gravitational potential) as tracer of the remnant dynamics
- Lapse low = compact, lapse large = less compact → increase = expansion

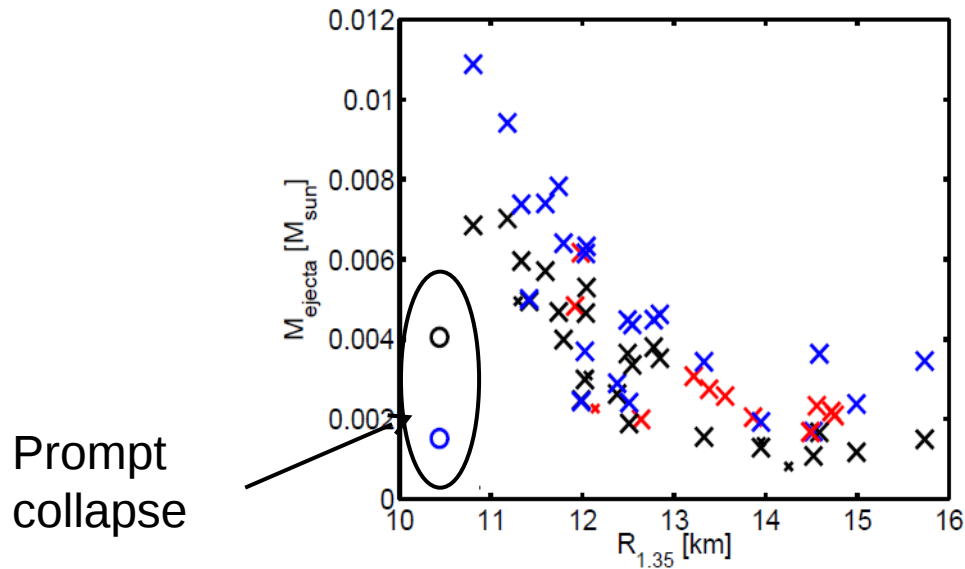


Bauswein et al. 2013

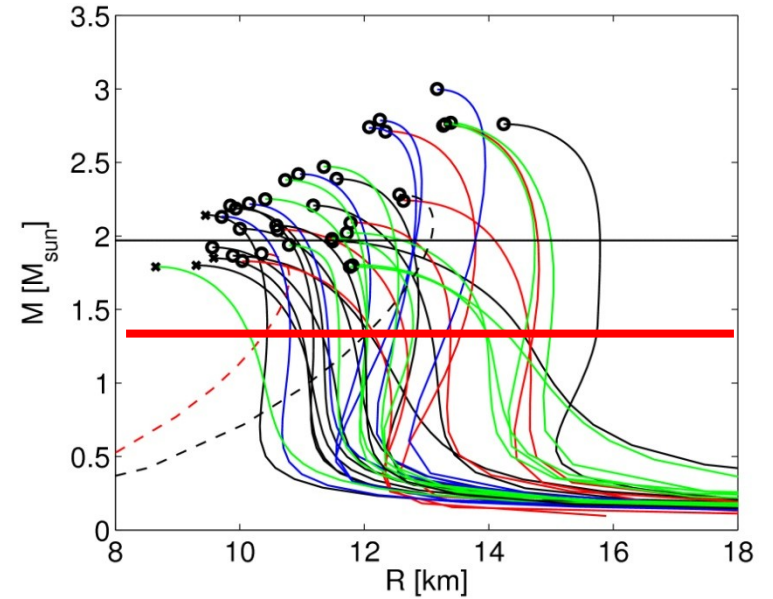
Stiffness of the EoS

Dashed line: central lapse, solid line: ejecta mass as function of time

Ejecta mass dependencies: EoS

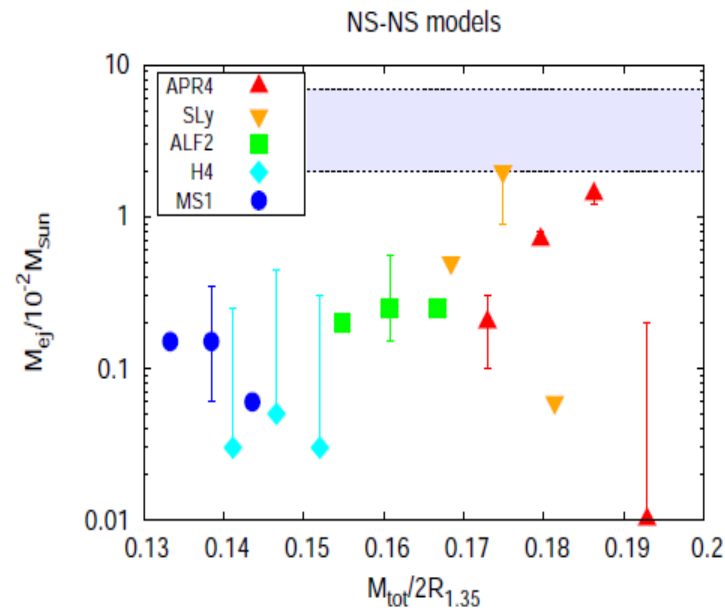


Bauswein et al 2013



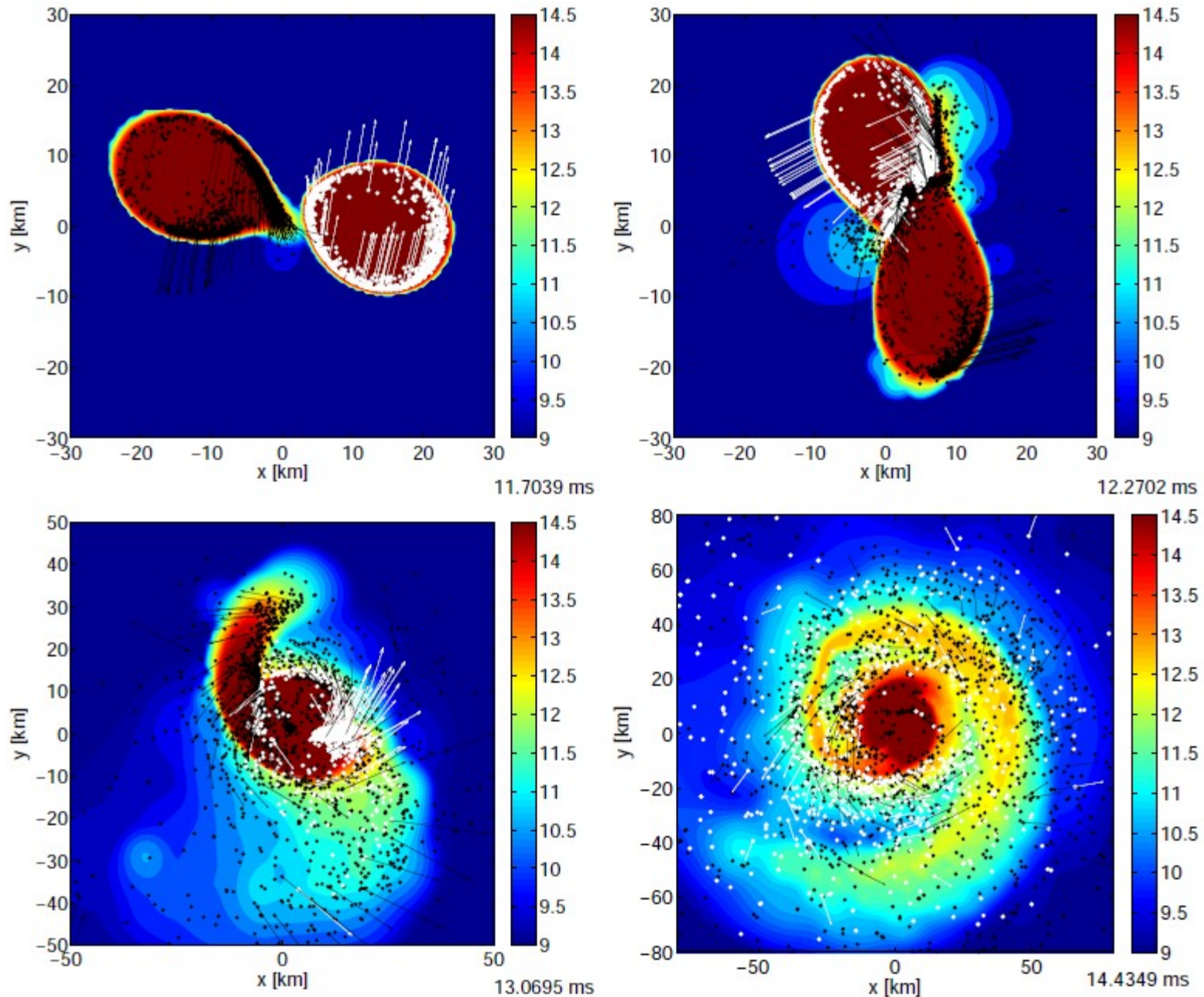
Note importance of thermal effects

1.35-1.35 M_{sun} binaries,
different EoSs



Hotokezaka et al 2013

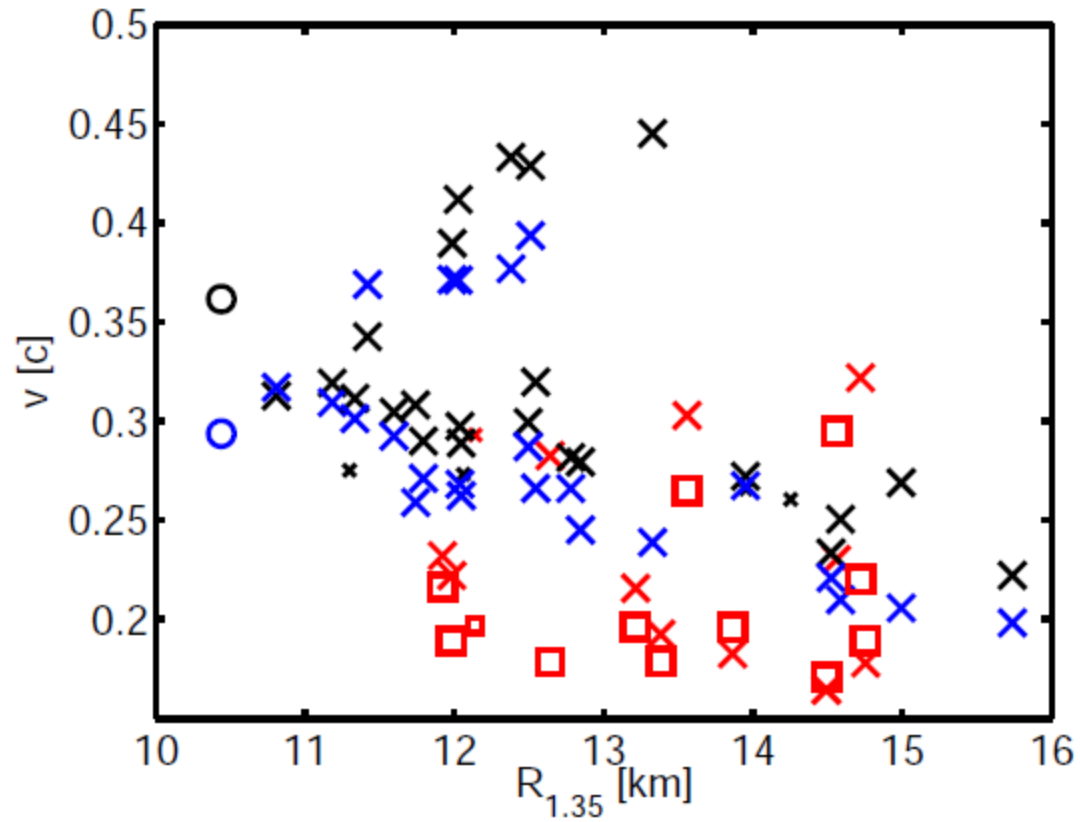
Asymmetric merger: 1.2-1.5 Msun



Bauswein et al. 2013

→ larger tidal component, larger masses

Ejecta velocities



Bauswein et al. 2013

Squares: 1.2-1.5 M_{sun}

Ejecta properties – nuclear network calculations

Robust features: **fast expansion, neutron rich** (neutrinos increase Y_e , see Wanajo et al. 2014, ...)

Originating from inner neutron crust 10^{14} g/cm³ (initial Y_e very low)

Matter heated to NSE and frozen out at \sim neutron drip $4 \cdot 10^{11}$ g/cm³

Ejecta expansion typically followed for a few 10 ms by simulations, then extrapolation (outcome insensitive), homologous expansion well justified

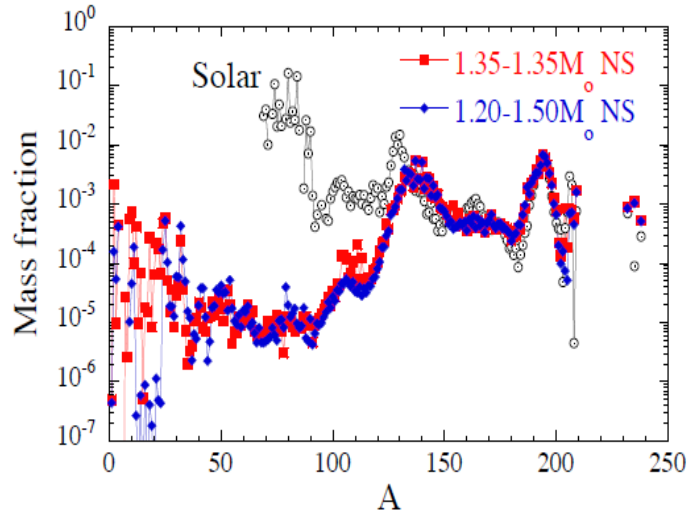
Post-processing hydrodynamical trajectories with nuclear network

- Properties of ~ 5000 nuclei (mostly theoretical models)
- Theoretical and experimental reaction rates: beta-decays, neutron captures, photodissociation, multiple-particle reactions (n,2n)
- Neutron-induced fission, spontaneous fission, beta-delayed fission, photofission, beta-delayed neutron emission
- Heating due to beta-decays, fission, alpha decays
- Note that nuclear physics are uncertain far away from valley of stability, mass model, reaction rates, fission yields

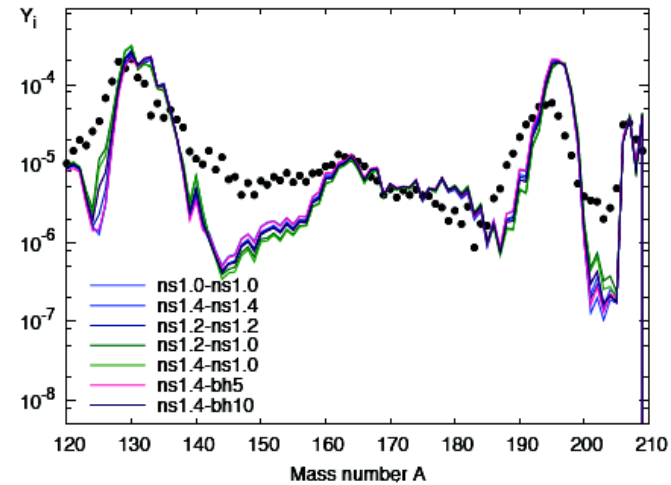
Nucleosynthesis results (dynamical ejecta)

Some recent results: different hydrodynamical models, different nuclear network codes, different NS EoS, different binary systems → **robust pattern (fission)**

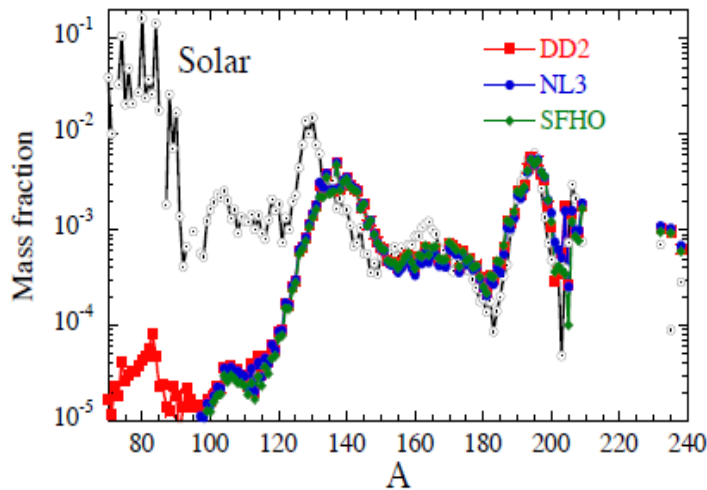
Black dots: observed abundances (results scaled)



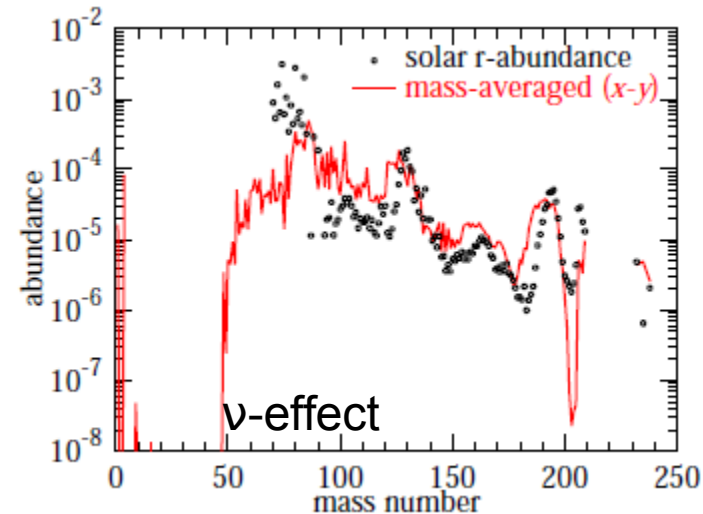
Goriely et al 2011



Korobkin et al. 2012



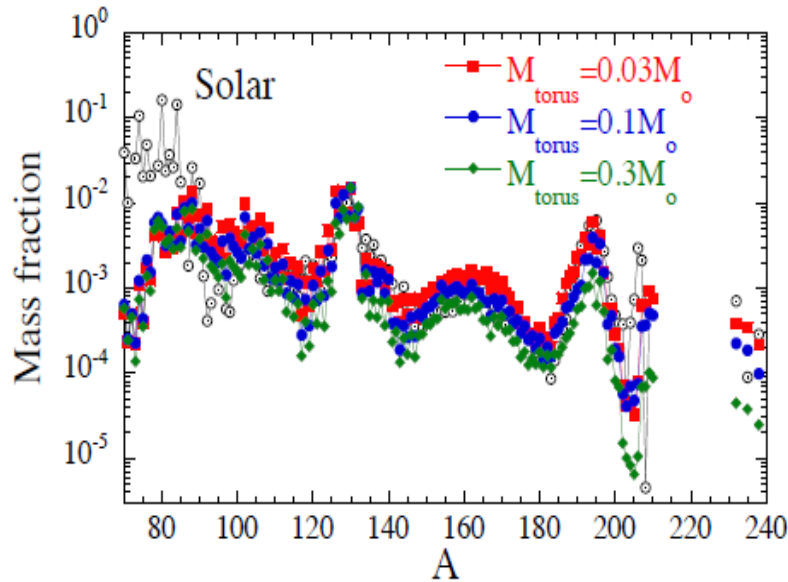
Bauswein et al 2013



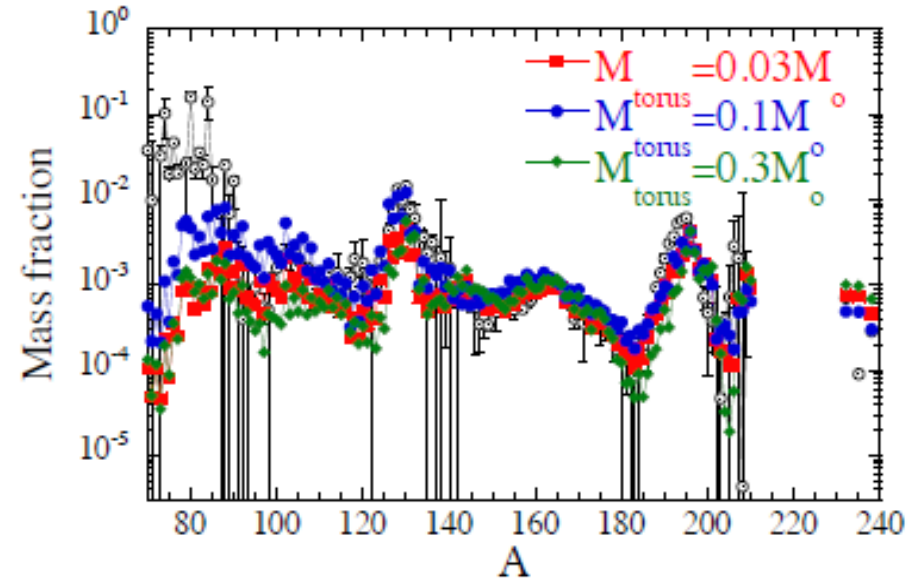
Wanajo et al. 2014

See also Freiburghaus et al 1999, Metzger et al. 2010, Roberts et al. 2011,...

Nucleosynthesis of secular ejecta



Only secular ejecta



Secular and dynamical ejecta
(merger and disk ejecta)

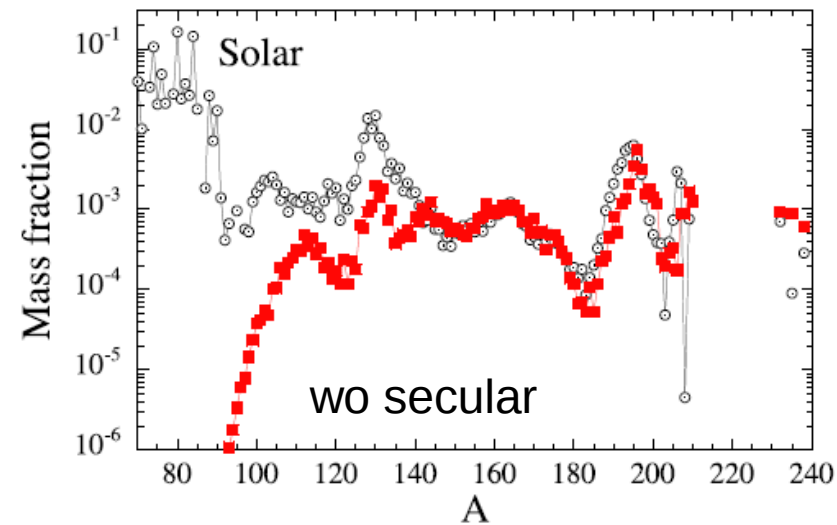
Just et al. 2014.

Mergers produce also the low A r-process elements

(similar for secular ejecta from long-lived NS remnant)

Note on NS-BH systems

- Can produce substantial amounts of dynamical ejecta (depending on system parameters)
- Time scales are similar to NSNS
- Tidal ejection (less affected by neutrinos)
 - very robust r-process, low S , low Y_e
 - fission cycling
- Resulting torus-BH
 - secular ejecta as for NSNS



Bauswein et al 2014

